SIAM J. SCI. COMPUT.
Vol. 41, No. 1, pp. A422–A451

AN ASYMPTOTIC-PRESERVING SCHEME FOR THE KINETIC EQUATION WITH ANISOTROPIC SCATTERING: HEAVY TAIL EQUILIBRIUM AND DEGENERATE COLLISION FREQUENCY*

LI WANG† AND BOKAI YAN‡

Abstract. We design an asymptotic preserving (AP) scheme for the linear kinetic equation with *anisotropic* scattering that leads to a fractional diffusion limit. This limit may be attributed to two reasons: a heavy tail equilibrium or a degenerate collision frequency, both of which are considered in this paper. Our scheme builds on the ideas developed in [L. Wang and B. Yan, *J. Comput. Phys.*, 312 (2016), pp. 157–174] but with *two major variations*. One is a *new* splitting of the system that accounts for the anisotropy in the scattering cross section by introducing two extra terms. We then showed, via detailed calculation, that the scheme enjoys a *relaxed* AP property as opposed to the one step AP for the isotropic scattering. Another contribution is for the degenerate collision frequency case, which brings in additional stiffness. We propose to integrate a "body" term, which appears to be the main component in the diffusion limit. This term is precomputed once with a prescribed accuracy, via a change of variable that alleviates the stiffness. Numerical examples are presented to validate its efficiency in both kinetic and fractional diffusion regimes.

Key words. fractional diffusion, asymptotic-preserving scheme, anisotropic scattering, heavy tail equilibrium, degenerate collision frequency

AMS subject classifications. 82C40, 82C80, 82D99, 65M06

DOI. 10.1137/17M1138029

1. Introduction.

In this paper, we consider the time evolution of the distribution function $f(t,x,v)$ which depends on time $t>0$, position $x\in\mathbf{R}^N$, and velocity $v\in\mathbf{R}^N$ and solves the following linear kinetic equation

$$\partial_t f + v\cdot\nabla_x f = \mathcal{L}(f), \qquad (t,x,v)\in(0,\infty)\times\mathbf{R}^N\times\mathbf{R}^N, \tag{1.1}$$

with the initial condition $f(0,x,v)=f_0(x,v)$. Here the collision operator $\mathcal{L}$ takes the form

$$\mathcal{L}(f)=\int_{\mathbf{R}^N}\phi(v,v')\left[\mathcal{M}(v)f(t,x,v')-\mathcal{M}(v')f(t,x,v)\right]\,\mathrm{d}v', \tag{1.2}$$

where $\phi(v,v')\geq 0$ is the scattering cross section symmetric in v and v': $\phi(v,v')=\phi(v',v)$, and $\mathcal{M}(v)\geq 0$ is the unique equilibrium satisfying [11, 19]

$$\mathcal{L}(\mathcal{M})=0, \qquad \mathcal{M}(v)=\mathcal{M}(-v), \qquad \int_{\mathbf{R}^N}\mathcal{M}(v)\,\mathrm{d}v=1 \quad \text{for all} \quad x\in\mathbf{R}^N. \tag{1.3}$$

In the cases when $\phi(v,v')\equiv 1$, the scattering becomes isotropic. Equations of this type take a wide range of applications in physics, examples including electron transport in

*Submitted to the journal's Methods and Algorithms for Scientific Computing section July 10, 2017; accepted for publication (in revised form) October 31, 2018; published electronically February 5, 2019.

http://www.siam.org/journals/sisc/41-1/M113802.html

Funding: The first author's work was partially supported by NSF grants DMS-1620135 and DMS-1903420.

†School of Mathematics, University of Minnesota Twin Cities, 206 Church St SE, Minneapolis, MN 55455 (wang8818@umn.edu).

‡Department of Mathematics, University of California, Los Angeles, 520 Portola Plaza, Los Angeles, CA 90095 (yanbokai@gmail.com).

semiconductor devices [21], evolution of plasmas [8, 7], fluxes of neutrons or photons [11], etc.

Conventionally, one can rewrite $\mathcal{L}(f)$ as

$$\mathcal{L}(f) = \mathcal{K}(f) - \nu(v) f\,, \tag{1.4}$$

where $\mathcal{K}(f)$ is the gain term defined as

$$\mathcal{K}(f) = \int_{\mathbf{R}^N} \phi(v, v') f(t, x, v')\, \mathrm{d}v' \mathcal{M}(v), \tag{1.5}$$

and $\nu(v)f$ is the loss term with

$$\nu(v) = \int_{\mathbf{R}^N} \phi(v, v') \mathcal{M}(v')\, \mathrm{d}v' \tag{1.6}$$

being the collision frequency. Typical macroscopic scaling of such equations is the diffusive scale, which leads to a diffusion equation. Specifically, the dimensionless form of (1.1), with a little abuse of notation, reads

$$\epsilon^\alpha \partial_t f + \epsilon v \cdot \nabla_x f = \mathcal{L}(f)\,, \tag{1.7}$$

where ϵ is the Knudsen number. It is well known that in the small mean free path ($\epsilon \ll 1$) and long time ($t \sim \epsilon^{-\alpha}$) regime with $\alpha = 2$, the distribution of the particles is at equilibrium given by a Maxwellian distribution function, and density, as the zeroth moment of f, solves a diffusion equation

$$\partial_t \rho - \nabla_x \cdot (\mathsf{D} \nabla_x \rho) = 0, \qquad \rho = \int_{\mathbf{R}^N} f\, \mathrm{d}v\,,$$

where D is the diffusion matrix

$$\mathsf{D} = \int_{\mathbf{R}^N} v \otimes \mathcal{L}^{-1}(v\mathcal{M})\, \mathrm{d}v. \tag{1.8}$$

The reader can reference [3, 6, 11, 18] for an extensive review of this limit.

However, such a limit fails when the diffusion matrix D becomes unbounded, which may be attributed to two different reasons. To explain, let us consider for now a simple case in which

$$\phi(v, v') = \frac{\nu(v)\nu(v')}{\langle \nu \mathcal{M} \rangle}\,; \tag{1.9}$$

then the collision $\mathcal{L}$ reduces to

$$\mathcal{L} f = \nu(v)(\rho_\nu \mathcal{M} - f), \quad \rho_\nu = \frac{\langle \nu f \rangle}{\langle \nu \mathcal{M} \rangle}, \tag{1.10}$$

and the diffusion matrix becomes

$$\mathsf{D} = \int_{\mathbf{R}^N} v \otimes v \frac{\mathcal{M}}{\nu(v)}\, \mathrm{d}v. \tag{1.11}$$

In the following, $\langle \cdot \rangle$ always denotes the average in the v direction, i.e., $\langle f \rangle = \int_{\mathbf{R}^N} f\, \mathrm{d}v$.

One reason that renders D infinite is due to the large velocity behavior of the equilibrium $\mathcal{M}$. When $\mathcal{M}$ is not a Maxwellian but rather a heavy tail function, i.e.,

$$\mathcal{M}^{\mathbf{t}}(v) = \begin{cases} \frac{\kappa_0}{|v|^{N+\alpha}} & \text{for } |v| \geq 1\,, \\ \kappa_0 & \text{for } 0 \leq |v| < 1\,, \end{cases} \qquad 0 < \alpha < 2\,, \tag{1.12}$$

then

$$\int v^2 \mathcal{M}^{\mathbf{t}} dv \sim \int_{|v|\geq 1} \frac{1}{|v|^{N+\alpha-2}}\, \mathrm{d}v = \infty\,, \tag{1.13}$$

and therefore D becomes infinite. Here we assume that ϕ is bounded from above and below. The equilibrium (1.12) arises in numerous areas of applications such as granular plasmas with dissipative collision [5, 8, 7, 13, 23], astrophysical plasmas [22], economy [12], and transport in atmospheric clouds [14]. See also [23] for a review of granular materials in which power law like distribution appears as a typical equilibrium in inelastic kinetic theory.

Another reason comes from the degeneracy in the collision frequency $\nu(v)$ when v is small. In particular, we assume that

$$\nu(v) = \nu_0 |v|^{N+2+\beta} \quad \text{for } |v| \leq \delta, \quad \beta > 0\,, \tag{1.14}$$

and let $\mathcal{M}$ be the classical Maxwellian or

$$\mathcal{M}^{\mathbf{d}}(v) = \begin{cases} M_0\,, & |v| \leq \delta\,, \\ 0\,, & \text{otherwise} \end{cases} \tag{1.15}$$

for simplicity, then $\mathsf{D} \sim M_0 \int_{|v|\leq\delta} |v|^{-N-\beta}\, \mathrm{d}v = \infty$. This case arises in the modeling of weak turbulence of chains of harmonic oscillators [4]. We use $\mathcal{M}^{\mathbf{t}}$ and $\mathcal{M}^{\mathbf{d}}$ to distinguish two different equilibria. Hereafter, we omit the superscript if the argument works for both cases. Similar notations apply to collision frequency ν and diffusion coefficient κ that appear later as well. For the degenerate case, we will restrict our attention to the specific case (1.9), and for the fat tail case, we will consider more general $\phi(v, v')$.

In either case the classical diffusion limit breaks down and one needs to consider a different time scale with $\alpha < 2$. The limiting behavior, as a result, is governed by a fractional diffusion equation. In the former case, a rigorous derivation is undertaken in [20] via the Fourier–Laplace transform and extended in [19] for a more general space dependent or anisotropic scattering based on a weak formulation and particular choice of test function. It is revisited in a more recent work [2] following a Hilbert expansion approach which is capable of proving strong convergence results. In the latter case, a weak convergence has been laid out in [1] via an auxiliary function.

Our goal in this paper is to design an efficient numerical method for the linear transport equation (1.1) wherein ϵ can take a wide range of magnitudes and $\alpha \neq 2$. A method of this type is coined as asymptotic preserving (AP) by Jin [16] since it preserves the corresponding asymptotic limit at the discrete level when mesh size and time step are kept fixed. As with analytical investigations, AP methods for (1.7) with classical diffusion scaling ($\alpha = 2$) are well developed (see [17] for a review), whereas there exist only a few methods for the anomalous diffusion. In [24], the authors designed an AP scheme for isotropic scattering (i.e., $\sigma(v, v')$ is independent of v or v, but may depend on x) with heavy tail equilibrium. The key ingredients there consist of a macro-micro decomposition that splits the kinetic equation following a reshuffled Hilbert expansion, and a tail compensation to account for the information lost in the overpopulated tail. In [10, 9], Crouseilles, Hivert, and Lemou developed three methods—a fully implicit scheme, a micro-macro decomposition based scheme, and a scheme using Duhamel formulation—for the special case: (1.9) with (1.14) for the degenerate collision frequency and (1.9) with $\nu \equiv 1$ for the heavy tail equilibrium case.

We intend to design a method that works for general scattering $\phi(v, v')$. The method we develop here builds on our previous work [24] but with substantial modification to handle the difficulties anisotropy brings in. As in [24], we first conduct a macro-micro decomposition. However, the main difficulty, in contrast with isotropic scattering, comes from the fact that we cannot simply split the gain and loss parts of the collision and distribute them into the macro and micro parts of the equation. To alleviate this issue, we propose *a variant of decomposition* such that the resulting system is well posed, at the cost of introducing two new terms $\langle \mathcal{K}(g) \rangle$ and $\langle \mathcal{K}(g) \rangle \mathcal{M}$. Consequently, instead of a strong AP property obtained in [24], we get a *relaxed-AP* property [25] here, meaning that the solution f will relax to the local equilibrium not in the first step but after a few steps. To extend the idea to the degenerate collision frequency case, the same system decomposition can be applied, but since equilibrium has a compact support in the velocity space, there is no need for tail compensation. Rather, we need to take care of the information for small velocity because (1) it makes the major contribution in the diffusion limit and (2) it brings singularity. Our new idea is to construct a precompute *integrated body* part. This can be accomplished by the change of variables, a procedure that was first proposed in analysis in [1] and has been implemented in numerics in [9].

The rest of the paper is organized as follows. In the next section we summarize the basic results regarding the fractional diffusion limit. The material is kept to a minimum to satisfy the needs in explaining the numerical methods that follow. Section 3 is devoted to the major part of our schemes. A system decomposition that suits both cases is presented first with a proof of its well-posedness. Then two different cases are considered separately. For the heavy tail equilibrium, we conduct a velocity truncation and tail compensation, whereas for the degenerate collision frequency, we perform a regular velocity discretization along with a special body integration. Numerical examples are given in section 4 to illustrate the efficiency of the new scheme. Finally the paper is concluded in section 5.

2. Fractional diffusion limit. In this section, we present a formal derivation of the fractional diffusion limit of (1.7) with the general collision (1.4) in two cases—heavy tail equilibrium and degenerate collision frequency, under the appropriate choice of time scale ϵ^α. Rigorous theory is available in [2, 19, 20] in the former case through various approaches including the Laplace–Fourier transform, moment method, and Hilbert expansion; whereas, in the latter case a weak convergence is obtained in [1] via an auxiliary function.

Our presentation here follows a reshuffled Hilbert expansion [2, 24]. Specifically, expand f as

$$f = f_0 + g_1 + g_2 + \cdots,$$

and plug it into (1.7) (1.4), then the leading terms are solved by

$$0 = \mathcal{L}(f_0), \tag{2.1}$$

$$\epsilon v \cdot \nabla_x (f_0 + g_1) = -\nu(v) g_1, \tag{2.2}$$

$$\epsilon^\alpha \partial_t f_0 = \mathcal{K}(g_1) + \mathcal{L}(g_2). \tag{2.3}$$

At variance with the classical diffusion limit, the terms $\mathcal{K}(g_1)$ and $\epsilon v \cdot \nabla_x g_1$ in (2.2), (2.3) swap places. This is inspired by the observation that when $\alpha > 1$ the gain term of the collision operator is of higher order than the loss term and the convection term [2]. From (2.1), one gets

$$f_0 = \rho_0 \mathcal{M}(v), \tag{2.4}$$

and the solvability condition in (2.3) yields

$$\epsilon^\alpha \partial_t \rho_0 = \langle \mathcal{K}(g_1) \rangle \,. \tag{2.5}$$

Now we take the Fourier transform in (2.2) with respect to x and get g_1. More precisely, denote $\hat{g}(t,k,v)$ as the Fourier transform of $g(t,x,v)$, i.e., $\hat{g} = \int_{\mathbf{R}^N} g e^{-ik\cdot x} dx$, then we have

$$(\nu(v) + i\epsilon v \cdot k)\hat{g_1} = -i\epsilon v \cdot k \hat{f}_0,$$

and thus

$$\hat{g}_1 = -\frac{i\epsilon v \cdot k}{\nu(v) + i\epsilon v \cdot k} \hat{f}_0 \,.$$

Similarly, we take the Fourier transform in (2.3) and integrate in v to get

$$\partial_t \hat{\rho}_0 = \frac{1}{\epsilon^\alpha} \langle \mathcal{K}(\hat{g}_1) \rangle \,, \tag{2.6}$$

where

$$\frac{1}{\epsilon^\alpha} \langle \mathcal{K}(\hat{g_1}) \rangle = \frac{1}{\epsilon^\alpha} \langle \nu \hat{g}_1 \rangle = -\frac{1}{\epsilon^\alpha} \int_{\mathbf{R}^N} \frac{i\epsilon v \cdot k}{\nu(v) + i\epsilon v \cdot k} \mathcal{M}(v) \nu(v) \, \mathrm{d}v \hat{\rho}_0 \,. \tag{2.7}$$

To proceed, we need to examine the integral in the last term of (2.7) with vanishing ϵ. This will be discussed separately for each cases.

2.1. Case I: Heavy tail equilibrium. In the case of heavy tail equilibrium, let us assume that

$$0 < \phi_0 \le \phi(v, v') \le \phi_1 \,, \tag{2.8}$$

and the equilibrium $\mathcal{M}^{\mathbf{t}}(v)$ takes the form (1.12) where κ_0 is chosen such that $\mathcal{M}^{\mathbf{t}}(v)$ integrates to one. We further assume that

$$\nu^{\mathbf{t}}(v) \to \nu_0 \quad \text{as } |v| \to \infty \,, \tag{2.9}$$

where $\nu^{\mathbf{t}}$ is defined in (1.6) with $\mathcal{M} = \mathcal{M}^{\mathbf{t}}$. First we recall a lemma from [24].

LEMMA 2.1 (see [24]). *Sending $\epsilon \to 0$, we have*

$$\frac{1}{\epsilon^\alpha} \int_{\mathbf{R}^N} \frac{i\epsilon v \cdot k \nu_0}{\nu_0 + i\epsilon v \cdot k} \mathcal{M}^{\mathbf{t}}(v) \, \mathrm{d}v \to \kappa^{\mathbf{t}} |k|^\alpha \tag{2.10}$$

with $\kappa^{\mathbf{t}}$ given by

$$\kappa^{\mathbf{t}} = \kappa_0 \nu_0 \int_{\mathbf{R}^N} \frac{(w \cdot e)^2}{\nu_0^2 + (w \cdot e)^2} \frac{1}{|w|^{N+\alpha}} \, \mathrm{d}w \,, \tag{2.11}$$

where e is an unit vector in $\mathbf{R}^N$.

Now it is obvious that, equipped with the above lemma, (2.6) in the zero limit of ϵ has the form of fractional diffusion. More precisely, we have the following.

THEOREM 2.2 (see [20]). *The solution f to (1.7) converges to $\rho(t,x)\mathcal{M}^{\mathbf{t}}(v)$ in $L^\infty(0,T;L^2(R^N\times R^N))$-weak, where $\rho(t,x)$ is the unique solution of the fractional diffusion equation*

$$\begin{cases} \partial_t\rho+\kappa^{\mathbf{t}}(-\Delta)^{\frac{\alpha}{2}}\rho=0,\\ \rho(x,0)=\rho_{in}(x)\end{cases} \tag{2.12}$$

with

$$\kappa^{\mathbf{t}}=\kappa_0\nu_0\int_{\mathbf{R}^N}\frac{(\omega\cdot e)^2}{\nu_0^2+(\omega\cdot e)^2}\frac{1}{|\omega|^{N+\alpha}}\,\mathrm{d}\omega\,, \tag{2.13}$$

where $e\in\mathbf{R}^N$ with $|e|=1$.

2.2. Case II: Degenerate collision frequency. When the collision frequency degenerates with small velocity, a fractional diffusion is also expected. In particular, we assume that $\mathcal{M}^{\mathbf{d}}(v)$ takes the form of (1.15) and consider the degenerate collision frequency (1.14), then we first have the following lemma regarding the integral in (2.7), and the proof herein provides some techniques that will be used in designing the numerical methods later on.

LEMMA 2.3. *Sending $\epsilon\to 0$, we have*

$$\frac{1}{\epsilon^\alpha}\int_{\mathbf{R}^N}\frac{i\epsilon v\cdot k}{\nu^{\mathbf{d}}(v)+i\epsilon v\cdot k}\nu(v)\mathcal{M}^{\mathbf{d}}(v)\,\mathrm{d}v\to\kappa^{\mathbf{d}}|k|^\alpha\,, \tag{2.14}$$

where $\nu(v)$ satisfies (1.14), $\mathcal{M}^{\mathbf{d}}(v)$, $\kappa^{\mathbf{d}}$, and α take the form (1.15), (2.21), and (2.19), respectively.

Proof. Using the form of $\mathcal{M}^{\mathbf{d}}(v)$ in (1.15), we have

$$\frac{1}{\epsilon^\alpha}\int_{\mathbf{R}^N}\frac{i\epsilon v\cdot k}{\nu^{\mathbf{d}}(v)+i\epsilon v\cdot k}\nu^{\mathbf{d}}(v)\mathcal{M}^{\mathbf{d}}(v)\,\mathrm{d}v=\epsilon^{2-\alpha}\int_{|v|\le\delta}\frac{(v\cdot k)^2M_0\nu^{\mathbf{d}}(v)}{\nu^{\mathbf{d}}(v)^2+(\epsilon v\cdot k)^2}\,\mathrm{d}v. \tag{2.15}$$

Denote

$$\gamma=N+1+\beta\,, \tag{2.16}$$

then upon changing variable

$$\omega=\frac{\epsilon|k|v}{\nu(v)}=\frac{\epsilon|k|v}{\nu_0|v|^{\gamma+1}}\,, \tag{2.17}$$

we have

$$|\omega|=\frac{\epsilon|k|}{\nu_0}|v|^{-\gamma},\quad \mathrm{d}v=\frac{1}{\gamma}\left(\frac{\epsilon|k|}{\nu_0|\omega|^{\gamma+1}}\right)^{N/\gamma}\mathrm{d}\omega\,, \tag{2.18}$$

and (2.15) becomes

$$\begin{aligned}&\epsilon^{2-\alpha}\int_{|\omega|\ge\frac{\epsilon|k|}{\nu_0\delta^\gamma}}\frac{M_0\left(\frac{\nu_0}{\epsilon}|v|^{\gamma+1}\omega\cdot e\right)^2}{(\nu_0|v|^{\gamma+1})^2+(\nu_0|v|^{\gamma+1}\omega\cdot e)^2}\frac{1}{\gamma}\left(\frac{\epsilon|k|}{\nu_0|\omega|^{\gamma+1}}\right)^{N/\gamma}\nu_0|v|^{1+\gamma}\,\mathrm{d}\omega\\ &=\frac{M_0\nu_0}{\gamma}\epsilon^{-\alpha}\int_{|\omega|\ge\frac{\epsilon|k|}{\nu_0\delta^\gamma}}\frac{(\omega\cdot e)^2}{1+(\omega\cdot e)^2}\left(\frac{\epsilon|k|}{\nu_0|\omega|^{\gamma+1}}\right)^{\frac{N}{\gamma}}\left(\frac{\epsilon|k|}{\nu_0|\omega|}\right)^{\frac{\gamma+1}{\gamma}}\mathrm{d}\omega\\ &=\frac{M_0\nu_0^{1-\alpha}}{\gamma}\int_{|\omega|\ge\frac{\epsilon|k|}{\nu_0\delta^\gamma}}\frac{(\omega\cdot e)^2}{1+(\omega\cdot e)^2}\frac{1}{|\omega|^{N+\alpha}}\,\mathrm{d}\omega|k|^\alpha\,,\end{aligned}$$

which converges to $\kappa^{\mathbf{d}}|k|^\alpha$ as $\epsilon \to 0$, where $\kappa^{\mathbf{d}}$ is defined in (2.21). Here e is again a unit vector in $\mathbf{R}^N$. ∎

Then we cite the following theorem from [1] but omit the details of the proof. Indeed, one major component in the proof has been outlined in the above lemma.

THEOREM 2.4 (see [1]). *Assume that* (1.14) *and* $\int_{|v|\geq\delta} \frac{|v|^2}{\nu(v)}\mathcal{M}^{\mathbf{d}}(v)\,\mathrm{d}v \leq +\infty$, $\int_{\mathbf{R}^N} \nu(v)^2\mathcal{M}^{\mathbf{d}}(v)dv \leq +\infty$ *hold, then the solution* f *of* (1.7) *with*

$$\alpha = \frac{\beta + 2N + 2}{\beta + N + 1} \tag{2.19}$$

converges weakly in $L^2_{\nu\mathcal{M}^{-1}}(\mathbf{R}^N \times \mathbf{R}^N \times (0,T))$ *to* $\rho(t,x)\mathcal{M}^{\mathbf{d}}(v)$, *where* $\rho(t,x)$ *solves*

$$\begin{cases} \partial_t\rho + \kappa^{\mathbf{d}}(-\Delta)^{\frac{\alpha}{2}}\rho = 0, \\ \rho(x,0) = \rho_{in}(x)\,, \end{cases} \tag{2.20}$$

and $\kappa^{\mathbf{d}}$ *is given by*

$$\kappa^{\mathbf{d}} = \frac{M_0\nu_0^{1-\alpha}}{1+N+\beta}\int_{\mathbf{R}^N}\frac{(w\cdot e)^2}{1+(w\cdot e)^2}\frac{1}{|w|^{N+\alpha}}\,\mathrm{d}w\,, \tag{2.21}$$

where $e \in \mathbf{R}^N$ *with* $|e| = 1$.

3. Numerical methods. In view of (1.7), the major challenge in numerical computation comes from the stiffness, which renders any explicit numerical schemes too expensive in the small ϵ limit. For this reason, an implicit treatment is often expected, but it always brings in another difficulty—a need to solve a large algebraic system. Our goal is to design a scheme that treats the stiff terms implicitly but does not generate any burden in inverting the resulting system. This is accomplished by the following two steps: a system decomposition, and a *tail/body* compensation in velocity discretization.

3.1. System decomposition. The first component in our scheme is the splitting of the original kinetic equation into two subequations, as is done in [24]. This is to distinguish different scales so that they can be treated in different manners. The main difference here as opposed to that in [24] is attributed to the anisotropy in the collision cross section, which introduces two extra terms in the splitting that need a special treatment. We will address this issue in the next subsection.

Recall the initial value problem

$$\begin{cases} \epsilon^\alpha\partial_t f + \epsilon v\cdot\nabla_x f = \mathcal{K}(f) - \nu(v)f, \\ f(0,x,v) = f_{\mathrm{in}}(x,v). \end{cases} \tag{3.1}$$

Decompose f into a macroscopic part and a microscopic part,

$$f(t,x,v) = \rho(t,x)\mathcal{M}(v) + g(t,x,v)\,, \tag{3.2}$$

where $\rho\mathcal{M}$ accounts for the equilibrium part and g characterizes the nonequilibrium perturbation. Note here that ρ is *not* the average of f for nonzero ϵ, i.e., $\rho \neq \langle f\rangle$ and $\langle g\rangle \neq 0$; only when $\epsilon \to 0$ do we have $\rho \to \langle f\rangle$ and $\langle g\rangle \to 0$.

Plugging (3.2) into (3.1), it can be rewritten as

$$\epsilon^\alpha\partial_t(\rho\mathcal{M}+g) + \epsilon v\cdot\nabla_x(\rho\mathcal{M}+g) = \mathcal{K}(\rho\mathcal{M}+g) - \nu(v)(\rho\mathcal{M}+g)\,,$$

which can be split into two subequations as suggested by the Hilbert expansion (2.1)–(2.3):

$$\epsilon^\alpha \partial_t \rho = \langle \mathcal{K}(g) \rangle \,, \tag{3.3}$$

$$\epsilon^\alpha \partial_t g + \epsilon v \cdot \nabla_x (\rho \mathcal{M} + g) = -\nu(v) g + \mathcal{K}(g) - \langle \mathcal{K}(g) \rangle \mathcal{M} \,. \tag{3.4}$$

As opposed to the isotropic case where ϕ is independent of v and v', here $\mathcal{K}(g) \neq \langle \mathcal{K}(g) \rangle \mathcal{M}$ in (3.4). Likewise, an initial value decomposition is chosen to be

$$\begin{cases} \rho_{\text{in}} = \dfrac{\langle \nu (f_{\text{in}} - g_{\text{in}}) \rangle}{\langle \nu \mathcal{M} \rangle} = \dfrac{\langle \nu f_{\text{in}} + \epsilon v \cdot \nabla_x f_{\text{in}} \rangle}{\langle \nu \mathcal{M} \rangle}, \\ g_{\text{in}} = f_{\text{in}} - \rho_{\text{in}} \mathcal{M}, \end{cases} \tag{3.5}$$

which is suggested from the observation that $\epsilon v \cdot \nabla_x (\rho \mathcal{M} + g) = -\nu(v) g$ holds in the limit of $\epsilon \to 0$. Then (3.3), (3.4) along with initial condition (3.5) constitute an alternative formulation for (3.1). To be more precise, we first have the following propositions regarding the relationship between the solutions to the original and decomposed systems. The results are similar to that in [24], but the proof is more involved.

PROPOSITION 3.1. *Let* (ρ, g) *be the solution to* (3.3), (3.4) *with initial data* (3.5), *then* $f = \rho \mathcal{M} + g$ *is a solution to* (3.1). *Denote the energy by*

$$E_f = \left(\iint f^2 \mathcal{M}^{-1} \, \mathrm{d}x \, \mathrm{d}v \right)^{1/2} = \left(\iint (\rho \mathcal{M} + g)^2 \mathcal{M}^{-1} \, \mathrm{d}x \, \mathrm{d}v \right)^{1/2}, \tag{3.6}$$

then both systems enjoy an energy dissipation $\frac{\mathrm{d}}{\mathrm{d}t} E_f \leq 0$.

Proof. It is easy to show that $f = \rho \mathcal{M} + g$ is a solution to (3.1) if (ρ, g) solve (3.3), (3.4) with initial data (3.5) by simply adding the equations, and energy dissipation (3.6) directly follows from an energy estimate. Indeed, multiplying (3.1) by $2 f \mathcal{M}^{-1}$ and integrating against both x and v, we have

$$\frac{\mathrm{d}}{\mathrm{d}t} \iint f^2 \mathcal{M}^{-1} \, \mathrm{d}x \, \mathrm{d}v = \frac{2}{\epsilon^\alpha} \iiint \phi(v, v') (f' \mathcal{M} - f \mathcal{M}') f \mathcal{M}^{-1} \, \mathrm{d}v \, \mathrm{d}v' \, \mathrm{d}x \,,$$

where f' and $\mathcal{M}'$ are short for $f(t, x, v')$ and $\mathcal{M}(t, x, v')$. Notice that

$$\begin{aligned} &2 \iiint \phi(v, v') (f' \mathcal{M} - f \mathcal{M}') f \mathcal{M}^{-1} \, \mathrm{d}v \, \mathrm{d}v' \, \mathrm{d}x \\ &\quad = - \iiint \left(\frac{f}{\mathcal{M}} - \frac{f'}{\mathcal{M}'} \right)^2 \phi(v, v') \mathcal{M} \mathcal{M}' \, \mathrm{d}v \, \mathrm{d}v' \, \mathrm{d}x \end{aligned} \tag{3.7}$$

and thus $\frac{\mathrm{d}}{\mathrm{d}t} \int f^2 \mathcal{M}^{-1} \, \mathrm{d}x \, \mathrm{d}v \leq 0$. Likewise, for the decomposed system (3.3), (3.4), multiplying (3.3) by $\rho \mathcal{M}$ and (3.4) by $g \mathcal{M}^{-1}$ and integrating both of them in x and v, we have the following equality by adding them together:

$$\begin{aligned} &\frac{1}{2} \iint \epsilon^\alpha \partial_t (\rho^2 \mathcal{M} + g^2 \mathcal{M}^{-1} + 2 \rho g) + \epsilon v \cdot \nabla_x (\rho \mathcal{M} + g) \frac{g}{\mathcal{M}} \, \mathrm{d}x \, \mathrm{d}v \\ &= \iint \langle \mathcal{K}(g) \rangle \rho \mathcal{M} - \nu \frac{g^2}{\mathcal{M}} + \mathcal{K}(g) \frac{g}{\mathcal{M}} - \langle \mathcal{K}(g) \rangle g \\ &\qquad + \langle \mathcal{K}(g) \rangle g - \nu \rho g - \epsilon v \cdot \nabla_x (\rho \mathcal{M} + g) \rho + \mathcal{K}(g) \rho - \langle \mathcal{K}(g) \rangle \mathcal{M} \rho \, \mathrm{d}x \, \mathrm{d}v \,. \end{aligned}$$

Notice that since $\iint v\cdot\nabla_x g\frac{g}{\mathcal{M}}\,\mathrm{d}x\,\mathrm{d}v=\iint v\cdot\nabla_x(\rho\mathcal{M})\rho\,\mathrm{d}x\,\mathrm{d}v=0$, it follows that

$$\begin{aligned}\frac{d}{dt}\iint(\rho^2\mathcal{M}+g^2\mathcal{M}^{-1}+2\rho g)\,\mathrm{d}x\,\mathrm{d}v&=\iint(\mathcal{K}(g)-\nu g)(\rho\mathcal{M}+g)\frac{1}{\mathcal{M}}\,\mathrm{d}x\,\mathrm{d}v\\&=\iint\mathcal{L}(f)f\frac{1}{\mathcal{M}}\,\mathrm{d}x\,\mathrm{d}v\le 0\,,\end{aligned}\tag{3.8}$$

where the last inequality comes from (3.7). ∎

Now we are in position to show that the decomposition (3.3), (3.4) is well-posed: the existence is obvious due to the linearity of the problem, and the stability is owing to the following proposition.

PROPOSITION 3.2. *Let (ρ,g) solve* (3.3), (3.4) *with initial data* (3.5), *then $\rho\in L^\infty(0,\infty;L^2(\mathbf{R}^N))$, $g\in L^\infty(0,\infty;L^2_{\mathcal{M}^{-1}}(\mathbf{R}^N\times\mathbf{R}^N))$. That is,*

$$E_\rho:=\left(\int\rho^2\,\mathrm{d}x\right)^{1/2}\quad\text{and}\quad E_g:=\left(\iint\frac{g^2}{\mathcal{M}}\,\mathrm{d}x\,\mathrm{d}v\right)^{1/2}\tag{3.9}$$

are both uniformly bounded in time.

Proof. Multiplying ρ on both sides of (3.3) and integrating over x, one has

$$\begin{aligned}\frac{1}{2}\epsilon^\alpha\frac{d}{dt}\int\rho^2\,\mathrm{d}x&=\int\rho\,\langle\mathcal{K}(g)\rangle\,\mathrm{d}x=\int\rho\iint\phi(v,v')(f-\rho\mathcal{M})\mathcal{M}'\,\mathrm{d}v'\,\mathrm{d}v\,\mathrm{d}x\\&=\iiint\phi\rho f\mathcal{M}'\,\mathrm{d}v'\,\mathrm{d}v\,\mathrm{d}x-\iiint\phi\rho^2\mathcal{M}\mathcal{M}'\,\mathrm{d}v'\,\mathrm{d}v\,\mathrm{d}x.\end{aligned}$$

Since $\phi(v,v')$ is uniformly bounded from above and below by (2.8) and f and $\mathcal{M}$ are both positive, the above equality has the following estimate:

$$\begin{aligned}&\frac{\epsilon^\alpha}{2}\frac{d}{dt}\int\rho^2\,\mathrm{d}x\le\phi_1\iiint|\rho|f\mathcal{M}'\,\mathrm{d}v'\,\mathrm{d}v\,\mathrm{d}x-\phi_0\iiint\rho^2\mathcal{M}\mathcal{M}'\,\mathrm{d}v'\,\mathrm{d}v\,\mathrm{d}x\\&=\phi_1\iint|\rho|f\,\mathrm{d}v\,\mathrm{d}x-\phi_0\int\rho^2dx\le\phi_1\left(\int\rho^2\,\mathrm{d}x\right)^{1/2}\left(\iint\frac{f^2}{\mathcal{M}}\,\mathrm{d}x\,\mathrm{d}v\right)^{1/2}-\phi_0\int\rho^2\,\mathrm{d}x\,.\end{aligned}$$

Rewriting it using the notation of (3.9), it condenses to

$$\frac{1}{2}\epsilon^\alpha\partial_t E_\rho^2\le\phi_1E_\rho E_f-\phi_0E_\rho^2$$

and, thus,

$$\epsilon^\alpha\partial_tE_\rho\le\phi_1E_f-\phi_0E_\rho\,.$$

Since E_f decays with time from Proposition 3.1, E_ρ is uniformly bounded in time. Note that

$$E_g^2=\iint(f-\rho\mathcal{M})^2\mathcal{M}^{-1}\,\mathrm{d}v\,\mathrm{d}x\le2\iint(f^2+(\rho\mathcal{M})^2)\mathcal{M}^{-1}\,\mathrm{d}v\,\mathrm{d}x=2(E_f^2+E_\rho^2);\tag{3.10}$$

therefore, E_g is also uniformly bounded in time. ∎

3.2. First order semidiscretization in time. This section is devoted to a first order temporal semidiscrete scheme based on the decomposition (3.3), (3.4). Specifically, we treat the stiff terms implicitly and the regular terms explicitly, and the scheme is written

$$\begin{cases} \epsilon^\alpha \dfrac{\rho^{n+1}-\rho^n}{\Delta t} = \left\langle \mathcal{K}(g^{n+1}) \right\rangle, \\ \epsilon^\alpha \dfrac{g^{n+1}-g^n}{\Delta t} + \epsilon v \cdot \nabla_x (\rho^* \mathcal{M} + g^{n+1}) = -\nu g^{n+1} + \mathcal{K}(g^n) - \left\langle \mathcal{K}(g^n) \right\rangle \mathcal{M}, \end{cases} \tag{3.11}$$

where the initial data are obtained by (3.5). Here ρ^* can be either ρ^{n+1} or ρ^n, leading to an implicit or explicit treatment of the fractional diffusion equation in the limit.

Now we provide a glimpse into the AP property. Taking the Fourier transform in (3.11) with respect to x, we have

$$\frac{\hat\rho^{n+1}-\hat\rho^n}{\Delta t} = \frac{1}{\epsilon^\alpha} \left\langle \mathcal{K}(\hat g^{n+1}) \right\rangle, \tag{3.12}$$

$$\epsilon^\alpha \frac{\hat g^{n+1}-\hat g^n}{\Delta t} + i\epsilon v \cdot k(\hat\rho^* \mathcal{M} + \hat g^{n+1}) = -\nu \hat g^{n+1} + \mathcal{K}(\hat g^n) - \left\langle \mathcal{K}(\hat g^n) \right\rangle \mathcal{M}, \tag{3.13}$$

where (3.13) yields

$$\begin{aligned} \hat g^{n+1} &= \frac{-i\epsilon v \cdot k \hat\rho^* \mathcal{M}}{\frac{\epsilon^\alpha}{\Delta t} + \nu + i\epsilon v \cdot k} + \frac{\frac{\epsilon^\alpha}{\Delta t} \hat g^n}{\frac{\epsilon^\alpha}{\Delta t} + \nu + i\epsilon v \cdot k} + \frac{\mathcal{K}(\hat g^n) - \left\langle \mathcal{K}(\hat g^n) \right\rangle \mathcal{M}}{\frac{\epsilon^\alpha}{\Delta t} + \nu + i\epsilon v \cdot k} \\ &:= \mathcal{A}\hat\rho^* + \mathcal{B}\hat g^n + \mathcal{C}\hat g^n . \end{aligned} \tag{3.14}$$

Here $\mathcal{A}$, $\mathcal{B}$, and $\mathcal{C}$ are three linear operators. In what follows, we will show that in both scenarios,

$$\frac{1}{\epsilon^\alpha} \left\langle \mathcal{K}(\hat g^{n+1}) \right\rangle \to -\kappa^\bullet |k|^\alpha \hat\rho^* \tag{3.15}$$

for fixed Δt with $\kappa^\bullet$ being either $\kappa^{\mathbf{t}}$ or $\kappa^{\mathbf{d}}$, and thus the limiting scheme in (3.12) solves the fractional diffusion equation.

For the ease of calculation, we only show the AP property for the special case when $\phi(v, v')$ takes the form of (1.9), and leave a remark for more general situations. Notice that for (1.9), the gain term in the collision simplifies to

$$\mathcal{K}(g) = \frac{\nu \mathcal{M}}{\langle \nu \mathcal{M} \rangle} \langle \nu g \rangle . \tag{3.16}$$

3.2.1. AP property: Heavy tail equilibrium. In the case of heavy tail equilibrium, we assume that $\phi_0 \le \phi(v, v') \le \phi_1$ and, since $\nu^{\mathbf{t}}(v) = \int_{\mathbf{R}^N} \phi(v, v') \mathcal{M}^{\mathbf{t}}(v') \, \mathrm{d}v'$, we immediately have $\phi_0 \le \nu^{\mathbf{t}}(v) \le \phi_1$. Then by taking the average in v of (3.13), one sees that

$$\left\langle \nu^{\mathbf{t}} g^{n+1} \right\rangle \sim \mathcal{O}(\epsilon^{\alpha'}) \quad \text{for any } n \ge 0, \quad \alpha' = \min\{\alpha, 1\}. \tag{3.17}$$

Therefore,

$$\left\langle \mathcal{K}(\hat g^n) \right\rangle = \left\langle \nu^{\mathbf{t}} \hat g^n \right\rangle \sim \mathcal{O}(\epsilon^{\alpha'}) \quad \text{and} \quad \mathcal{K}(\hat g^n) = \frac{\nu^{\mathbf{t}} \mathcal{M}^{\mathbf{t}}}{\langle \nu^{\mathbf{t}} \mathcal{M}^{\mathbf{t}} \rangle} \left\langle \nu^{\mathbf{t}} \hat g^n \right\rangle \sim \mathcal{O}(\epsilon^{\alpha'}), \tag{3.18}$$

and consequently from (3.14),

$$\hat{g}^{n+1} \sim \mathcal{O}(\epsilon^{\alpha'}), \tag{3.19}$$

thanks again to the boundedness of $\nu^{\mathbf{t}}$. Then we can check that

$$\frac{1}{\epsilon^\alpha}\left\langle \mathcal{K}\left(\mathcal{B}\hat{g}^n\right)\right\rangle = \frac{1}{\epsilon^\alpha}\left\langle \nu^{\mathbf{t}}\mathcal{B}\hat{g}^n\right\rangle = \left\langle \frac{\frac{1}{\Delta t}\nu^{\mathbf{t}}\hat{g}^n}{\frac{\epsilon^\alpha}{\Delta t}+\nu^{\mathbf{t}}+i\epsilon v\cdot k}\right\rangle \to 0 \quad \text{as } \epsilon\to 0. \tag{3.20}$$

For $\mathcal{C}\hat{g}^n$, notice that

$$\begin{aligned}\frac{1}{\epsilon^\alpha}\left\langle \mathcal{K}(\mathcal{C}\hat{g}^n)\right\rangle &= \frac{1}{\epsilon^\alpha}\int_{\mathbf{R}^N}\nu^{\mathbf{t}}\mathcal{C}\hat{g}^n\,\mathrm{d}v = \frac{1}{\epsilon^\alpha}\int_{\mathbf{R}^N}\nu^{\mathbf{t}}\mathcal{C}\hat{g}^n - \left(\frac{\nu^{\mathbf{t}}\mathcal{M}^{\mathbf{t}}}{\langle\nu^{\mathbf{t}}\mathcal{M}^{\mathbf{t}}\rangle}-\mathcal{M}^{\mathbf{t}}\right)\left\langle\nu^{\mathbf{t}}\hat{g}^n\right\rangle\,\mathrm{d}v\\ &= \frac{1}{\epsilon^\alpha}\int_{\mathbf{R}^N}\left\langle\nu^{\mathbf{t}}\hat{g}^n\right\rangle\left[\frac{\frac{\nu\mathcal{M}^{\mathbf{t}}}{\langle\nu\mathcal{M}^{\mathbf{t}}\rangle}-\mathcal{M}^{\mathbf{t}}}{\frac{\epsilon^\alpha}{\Delta t}+\nu^{\mathbf{t}}+i\epsilon v\cdot k}\nu^{\mathbf{t}} - \left(\frac{\nu^{\mathbf{t}}\mathcal{M}^{\mathbf{t}}}{\langle\nu\mathcal{M}^{\mathbf{t}}\rangle}-\mathcal{M}^{\mathbf{t}}\right)\right]\mathrm{d}v\\ &= -\frac{\left\langle\nu^{\mathbf{t}}\hat{g}^n\right\rangle}{\epsilon^\alpha}\int_{\mathbf{R}^N}\frac{\frac{\epsilon^\alpha}{\Delta t}+i\epsilon v\cdot k}{\frac{\epsilon^\alpha}{\Delta t}+\nu^{\mathbf{t}}+i\epsilon v\cdot k}\left(\frac{\nu^{\mathbf{t}}\mathcal{M}^{\mathbf{t}}}{\langle\nu\mathcal{M}^{\mathbf{t}}\rangle}-\mathcal{M}^{\mathbf{t}}\right)\mathrm{d}v. \end{aligned} \tag{3.21}$$

Then from the fact that $\frac{\frac{\epsilon^\alpha}{\Delta t}+i\epsilon v\cdot k}{\frac{\epsilon^\alpha}{\Delta t}+\nu^{\mathbf{t}}+i\epsilon v\cdot k} \sim \mathcal{O}(\epsilon^{\alpha'})$ and (3.17), and $0<\alpha<2$, (3.21) vanishes in the zero limit of ϵ.

For $\mathcal{A}\hat{\rho}^*$, we have

$$\frac{1}{\epsilon^\alpha}\left\langle\mathcal{K}(\mathcal{A}\hat{\rho}^*)\right\rangle = \frac{1}{\epsilon^\alpha}\left\langle\nu^{\mathbf{t}}\mathcal{A}\hat{\rho}^*\right\rangle = \frac{1}{\epsilon^\alpha}\int_{\mathbf{R}^N}\frac{-\epsilon v\cdot ik\hat{\rho}^*}{\frac{\epsilon^\alpha}{\Delta t}+\nu^{\mathbf{t}}+\epsilon v\cdot ik}\nu^{\mathbf{t}}(v)\mathcal{M}^{\mathbf{t}}(v)\,\mathrm{d}v,$$

whose limit becomes

$$\lim_{\epsilon\to 0}\frac{1}{\epsilon^\alpha}\left\langle\mathcal{K}(\mathcal{A}\hat{\rho}^*)\right\rangle = \lim_{\epsilon\to 0}\frac{1}{\epsilon^\alpha}\int_{\mathbf{R}^N}\frac{-(\epsilon v\cdot k)^2}{{\nu^{\mathbf{t}}}^2+(\epsilon v\cdot k)^2}\nu^{\mathbf{t}}(v)\mathcal{M}^{\mathbf{t}}(v)\,\mathrm{d}v\hat{\rho}^* = -\kappa^{\mathbf{t}}|k|^\alpha\hat{\rho}^*, \tag{3.22}$$

where $\kappa^{\mathbf{t}}$ is given by (2.11). Plugging (3.22) into the Fourier transform of the first equation in (3.11), one obtains, as $\epsilon\to 0$,

$$\frac{\hat{\rho}^{n+1}-\hat{\rho}^n}{\Delta t} = \epsilon^{-\alpha}\left\langle\mathcal{K}\hat{g}^{n+1}\right\rangle = -\kappa^{\mathbf{t}}|k|^\alpha\hat{\rho}^*, \quad n\geq 1,$$

which gives a first order discretization of the limit equation (2.12).

Remark 3.3. The assumption (1.9) is not mandatory here. For the general case without this assumption, we can get a relaxed-AP property, a concept put forward in [25], meaning that the AP property is satisfied after an initial transition time. Then similarly to what is done in the next section, we don't show that $\frac{1}{\epsilon^\alpha}\left\langle\mathcal{K}\left(\mathcal{B}\hat{g}^n\right)\right\rangle\to 0$ or $\frac{1}{\epsilon^\alpha}\left\langle\mathcal{K}\left(\mathcal{C}\hat{g}^n\right)\right\rangle\to 0$, but rather get a result similar to Proposition 3.4.

3.2.2. AP property: Degenerate collision frequency. When the collision frequency $\nu(v)$ degenerates to zero at small velocity, it poses a singularity in the denominator of (3.14), thus all the estimates (3.17)–(3.19) in the first case cannot apply here, and more detailed analysis is needed.

In fact, we show below that we only get a relaxed-AP property rather than the strong AP property in the heavy tail case. The difference is that, given nonequilibrium initial data, a relaxed-AP scheme takes a few steps to converge to the local equilibrium

with an asymptotic error depending on the scale parameter, whereas for a strong AP scheme, it only takes one step. Coming back to our problem, it means that we need to allow the scheme (3.11) to run a few time steps before it reduces to the solver for the limiting fractional diffusion equation.

More specifically, we start with the form (3.14), and let $\hat{\rho}^*$ be $\hat{\rho}^{n+1}$, i.e.,

$$\hat{g}^{n+1} = \mathcal{A}\hat{\rho}^{n+1} + \mathcal{B}\hat{g}^n + \mathcal{C}\hat{g}^n\,.$$

The case with $\hat{\rho}^* = \hat{\rho}^n$ can be proved in exactly the same way. Now let us march one step forward to get

$$\hat{g}^{n+2} = \mathcal{A}\hat{\rho}^{n+2} + \mathcal{B}(\mathcal{A}\hat{\rho}^{n+1} + \mathcal{B}\hat{g}^n + \mathcal{C}\hat{g}^n) + \mathcal{C}\left(\mathcal{A}\hat{\rho}^{n+1} + \mathcal{B}\hat{g}^n + \mathcal{C}\hat{g}^n\right),$$

and then one step further to arrive at

$$\begin{aligned}\hat{g}^{n+3} = {} & \mathcal{A}\hat{\rho}^{n+3} + \mathcal{B}(\mathcal{A}\hat{\rho}^{n+2} + \mathcal{B}\mathcal{A}\hat{\rho}^{n+1} + \mathcal{B}^2\hat{g}^n + \mathcal{B}\mathcal{C}\hat{g}^n + \mathcal{C}\mathcal{A}\hat{\rho}^{n+1} + \mathcal{C}\mathcal{B}\hat{g}^n + \mathcal{C}^2\hat{g}^n) \\ & + \mathcal{C}(\mathcal{A}\hat{\rho}^{n+2} + \mathcal{B}\mathcal{A}\hat{\rho}^{n+1} + \mathcal{B}^2\hat{g}^n + \mathcal{B}\mathcal{C}\hat{g}^n + \mathcal{C}\mathcal{A}\hat{\rho}^{n+1} + \mathcal{C}\mathcal{B}\hat{g}^n + \mathcal{C}^2\hat{g}^n)\,. \end{aligned} \tag{3.23}$$

Now it amounts to showing that $\frac{1}{\epsilon^\alpha}\left\langle \mathcal{K}(\hat{g}^{n+3})\right\rangle \to -\kappa^{\mathbf{d}}|k|^\alpha\hat{\rho}^{n+3}$. Note from Lemma 2.3 that

$$\frac{1}{\epsilon^\alpha}\left\langle \mathcal{K}(\mathcal{A}\hat{\rho}^{n+3})\right\rangle = \frac{1}{\epsilon^\alpha}\left\langle \nu^{\mathbf{d}}\mathcal{A}\hat{\rho}^{n+3}\right\rangle \to \kappa^{\mathbf{d}}|k|^\alpha\hat{\rho}^{n+3} \quad \text{as } \epsilon\to 0\,. \tag{3.24}$$

Therefore, it remains to show that all the remaining terms, upon applying operator $\mathcal{K}$, taking the average in v, and dividing by ϵ^α, vanish in the zero limit of ϵ. We summarize the results in the following proposition and leave the proof to the appendix.

PROPOSITION 3.4. *Consider a fixed time step Δt.*

(1) *If initially $\hat{\rho}^0$ and $\hat{g}^0$ are bounded, then $\hat{g}^n$ obtained from* (3.13) *is uniformly bounded in ϵ.*

(2) *For $\forall n \geq 1$, we have*

$$\lim_{\epsilon\to 0}\left|\frac{1}{\epsilon^\alpha}\left\langle \mathcal{K}(\mathcal{B}\mathcal{A}\hat{\rho}^n)\right\rangle\right| = 0,\ \lim_{\epsilon\to 0}\left|\frac{1}{\epsilon^\alpha}\left\langle \mathcal{K}(\mathcal{B}^3\hat{g}^n)\right\rangle\right| = 0,\ \lim_{\epsilon\to 0}\left|\frac{1}{\epsilon^\alpha}\left\langle \mathcal{K}(\mathcal{B}^2\mathcal{C}\hat{g}^n)\right\rangle\right| = 0,$$
$$\lim_{\epsilon\to 0}\left|\frac{1}{\epsilon^\alpha}\left\langle \mathcal{K}(\mathcal{C}\mathcal{A}\hat{\rho}^n)\right\rangle\right| = 0,\ \lim_{\epsilon\to 0}\left|\frac{1}{\epsilon^\alpha}\left\langle \mathcal{K}(\mathcal{B}\mathcal{C}^2\hat{g}^n)\right\rangle\right| = 0\,.$$

(3) *For big enough m and $\forall n \geq 1$, $\lim_{\epsilon\to 0}\frac{1}{\epsilon^\alpha}\left\langle \mathcal{K}(\mathcal{C}^m\hat{\rho}^n)\right\rangle = 0$.*

This proposition does not include all terms in (3.23), for those terms that do not appear here can be estimated in a similar way. Details are available in the appendix.

Remark 3.5. For a relaxed AP scheme, one can use a successive time discretization to accelerate the convergence, as described in [25]. In particular, we can reformulate (3.11) into

$$\begin{cases} \epsilon^\alpha\dfrac{\rho^{n+1}-\rho^n}{\Delta t} = \left\langle \mathcal{K}(g^{n+1})\right\rangle, \\ \epsilon^\alpha\dfrac{g^*-g^n}{\Delta t} = \mathcal{K}(g^n) - \left\langle \mathcal{K}(g^n)\right\rangle\mathcal{M}, \\ \epsilon^\alpha\dfrac{g^{n+1,1}-g^*}{\Delta t/k} + \epsilon v\cdot\nabla_x(\rho^{n+1}\mathcal{M} + g^{n+1,1}) = -\nu g^{n+1,1}, \\ \qquad\qquad\qquad\qquad \vdots \\ \epsilon^\alpha\dfrac{g^{n+1}-g^{n+1,k-1}}{\Delta t/k} + \epsilon v\cdot\nabla_x(\rho^{n+1}\mathcal{M} + g^{n+1}) = -\nu g^{n+1}\,. \end{cases}$$

3.3. Numerical scheme: Heavy tail equilibrium.

3.3.1. Velocity truncation. Similarly to the isotropic scattering in [24], we need to consider the truncation in the velocity space as well as a special treatment for the tail such that it is computationally affordable and numerically accurate. To this end, we further decompose $\mathcal{M}^{\mathbf{t}}$ and g into

$$\mathcal{M}^{\mathbf{t}}(v) = \mathcal{M}^{\mathbf{t}}_{B}(v) + \mathcal{M}^{\mathbf{t}}_{T}(v), \quad g(t,x,v) = g_{B}(t,x,v) + g_{T}(t,x,v), \tag{3.25}$$

where $\mathcal{M}^{\mathbf{t}}_{B}$ and g_{B} support on the domain of $|v| \le v_{\max}$ representing the "body" part, whereas $\mathcal{M}^{\mathbf{t}}_{T}$ and g_{T} support on $|v| > v_{\max}$ representing the "tail" effect, i.e.,

$$\begin{aligned} &\mathcal{M}^{\mathbf{t}}_{B}(v) = \mathcal{M}^{\mathbf{t}}(v)\mathbf{1}_{|v|\le v_{\max}}, \qquad \mathcal{M}^{\mathbf{t}}_{T}(v) = \mathcal{M}^{\mathbf{t}}(v)\mathbf{1}_{|v|> v_{\max}}, \\ &g_{B}(v) = g(v)\mathbf{1}_{|v|\le v_{\max}}, \qquad g_{T}(v) = g(v)\mathbf{1}_{|v|> v_{\max}}. \end{aligned} \tag{3.26}$$

Likewise, let

$$v_{B} = v\mathbf{1}_{|v|\le v_{\max}}, \qquad v_{T} = v\mathbf{1}_{|v|> v_{\max}}. \tag{3.27}$$

Equations (3.3), (3.4) are then rewrittten

$$\epsilon^{\alpha}\partial_t \rho = \left\langle \nu^{\mathbf{t}}_{B} g_{B} \right\rangle + \left\langle \nu^{\mathbf{t}}_{T} g_{T} \right\rangle, \tag{3.28}$$

$$\epsilon^{\alpha}\partial_t g_{B} + \epsilon v\cdot\nabla_x(\rho\mathcal{M}_{B} + g_{B}) = -\nu^{\mathbf{t}}_{B} g_{B} + \mathcal{K}(g)\big|_{B} - \langle \mathcal{K}(g)\rangle \mathcal{M}^{\mathbf{t}}_{B}, \tag{3.29}$$

$$\epsilon^{\alpha}\partial_t g_{T} + \epsilon v\cdot\nabla_x(\rho\mathcal{M}_{T} + g_{T}) = -\nu^{\mathbf{t}}_{T} g_{T} + \mathcal{K}(g)\big|_{T} - \langle \mathcal{K}(g)\rangle \mathcal{M}^{\mathbf{t}}_{T}. \tag{3.30}$$

As written, (3.28)–(3.30) cannot be practically solved with ease. In a grid based numerical method one needs to truncate the velocity space at $|v| < v_{\max}$ and place a finite number of points in $[-v_{\max}, v_{\max}]$. Therefore all the integrations appearing here will be approximated by the integration in the truncated domain, and the tail g_{T} has to be approximated in an integrated manner. More precisely, we propose the following ideas (here we write everything in the continuous sense and, in implementation, the integration is done with the quadrature rule, and we use the midpoint rule with uniform grid in this paper):

- $\nu^{\mathbf{t}}_{B}$ in (3.29) is approximated by

$$\nu^{\mathbf{t}}_{B}(v) \simeq \int \phi(v_{B}, v'_{B})\mathcal{M}^{\mathbf{t}}_{B}\,\mathrm{d}v'. \tag{3.31}$$

  Compared to its exact value $\nu^{\mathbf{t}}_{B} = \int \phi(v_{B}, v')\mathcal{M}^{\mathbf{t}} dv'$, this approximation introduces an error

$$\mathrm{error}_{\nu^{\mathbf{t}}{}_{B}} = \int \phi(v_{B}, v'_{T})\mathcal{M}^{\mathbf{t}}_{T}\,\mathrm{d}v'. \tag{3.32}$$

- $\mathcal{K}(g)\big|_{B}$ in (3.29) is computed via

$$\mathcal{K}(g)\big|_{B} = \int \phi(v_{B}, v'_{B}) g'_{B}\,\mathrm{d}v'\mathcal{M}^{\mathbf{t}}_{B} \tag{3.33}$$

  which compared with its true value $\mathcal{K}(g)_{B} = \int \phi(v_{B}, v') g'\,\mathrm{d}v'\mathcal{M}^{\mathbf{t}}_{B}$, introduces an error

$$\mathrm{error}_{\mathcal{K}(g)_{B}} = \int \phi(v_{B}, v'_{T}) g'_{T}\,\mathrm{d}v'\mathcal{M}^{\mathbf{t}}_{B}. \tag{3.34}$$

- Given the above calculation, $\langle \mathcal{K}(g) \rangle$ in (3.29) is then computed as

$$\langle \mathcal{K}(g) \rangle = \iint \phi(v_{_B}, v'_{_B}) g'_{_B} \, \mathrm{d}v' \mathcal{M}^{\mathbf{t}}_{_B} \, \mathrm{d}v \,, \tag{3.35}$$

  which introduces the following error,

$$\begin{aligned} \mathrm{error}_{\langle \mathcal{K}(g) \rangle} = & \int \phi(v_B, v'_T) g'_T \, \mathrm{d}v' \mathcal{M}_B dv + \int \phi(v_T, v'_T) g'_T dv' \mathcal{M}_T \, \mathrm{d}v \\ & + \int \phi(v_T, v'_B) g'_B \, \mathrm{d}v' \mathcal{M}_T \, \mathrm{d}v \end{aligned} \tag{3.36}$$

  as compared to the true value $\langle \mathcal{K}(g) \rangle$.

- $\mathcal{M}^{\mathbf{t}}_{_B}$ in (3.29) is replaced by $\frac{\mathcal{M}^{\mathbf{t}}_{_B}}{\langle \mathcal{M}^{\mathbf{t}}_{_B} \rangle}$ to guarantee conservation of total mass upon integration in v and x, and the error we introduce here is

$$\mathrm{error}_{\mathcal{M}^{\mathbf{t}}_{_B}} = \frac{\mathcal{M}^{\mathbf{t}}_{_B}}{\langle \mathcal{M}^{\mathbf{t}}_{_B} \rangle} (\langle \mathcal{M}^{\mathbf{t}}_{_B} \rangle - 1) \,. \tag{3.37}$$

- For the tail $g_{_T}$, like in the isotropic case [24], is approximated by its "local equilibrium." In particular, it solves

$$\epsilon v \cdot \nabla_x (\rho \mathcal{M}^{\mathbf{t}}{}_{_T} + g_{_T}) = -\nu^{\mathbf{t}}_{_T} g_{_T}.$$

  Now applying the Fourier transform in x, the functions with a hat depend on the frequency variable k. Hence the average $\langle \nu^{\mathbf{t}}_{_T} \hat{g}_{_T} \rangle$ is given by

$$\begin{aligned} \frac{1}{\epsilon^\alpha} \langle \nu^{\mathbf{t}}_{_T} \hat{g}_{_T} \rangle &= -\frac{1}{\epsilon^\alpha} \int_{|v| \geq v_{\max}} \frac{i\epsilon v \cdot k \nu^{\mathbf{t}}_{_T}}{\nu^{\mathbf{t}}_{_T} + i\epsilon v \cdot k} \mathcal{M}^{\mathbf{t}}_{_T}(v) \, \mathrm{d}v \hat{\rho} \\ &= -\frac{1}{\epsilon^\alpha} \int_{|v| \geq v_{\max}} \frac{\nu^{\mathbf{t}}_{_T} (\epsilon v \cdot k)^2}{{\nu^{\mathbf{t}}_{_T}}^2 + (\epsilon v \cdot k)^2} \frac{\kappa_0}{|v|^{N+\alpha}} \, \mathrm{d}v \hat{\rho} := -C_\epsilon(k) \hat{\rho}, \end{aligned} \tag{3.38}$$

  where $C_\epsilon(k)$ is *precomputed* numerically with any accuracy, since $\alpha \leq 2$, and $v_{\max}$ is independent of ϵ (see (3.39) below). We would like to mention that approximating $g_{_T}$ by its local equilibrium is valid only when ϵ is small, therefore, when we pick $v_{\max}$, we will make sure that the tail itself is controlled by $\mathcal{O}(\Delta t)$ so that when ϵ is not small, the wrong computation of the tail part will only generate error that is comparable to the numerical error by using finite difference in time. It is also important to point out that $C_\epsilon(k) \to \kappa^{\mathbf{t}} |k|^\alpha$ as $\epsilon \to 0$, as one would expect.

All the above arguments are lumped into the following criteria of choosing $v_{\max}$. We need the errors $\mathrm{error}_{\nu^{\mathbf{t}}{}_{_B}}$, $\mathrm{error}_{\mathcal{K}(g)_{_B}}$, $\mathrm{error}_{\langle \mathcal{K}(g) \rangle}$, $\mathrm{error}_{\mathcal{M}^{\mathbf{t}}_{_B}}$ in (3.32), (3.34), (3.36), (3.37) to be bounded by δ, and $\frac{1}{\epsilon^\alpha} \langle \nu^{\mathbf{d}}_T g_{_T} \rangle$ should be of $\mathcal{O}(\delta)$ when $\epsilon \sim \mathcal{O}(1)$. As a consequence, we have

$$\int_{|v| > v_{\max}} \mathcal{M}^{\mathbf{t}} \, \mathrm{d}v < \delta \tag{3.39}$$

and, thus, in a first order method, $\delta = \mathcal{O}(\Delta t)$. Note specifically that $v_{\max}$ is *independent* of ϵ. When $\epsilon \ll 1$, the tail part $\langle \nu^{\mathbf{t}}_{_T} g_{_T} \rangle$ in (3.28) dominates over the body part $\langle \nu^{\mathbf{t}}_{_B} g_{_B} \rangle$ (see the derivation of the limit (2.10) in [24]) and gives a correct compensation to the limit equation (3.28). Altogether, an AP property guarantees both the uniform stability and uniform accuracy of our scheme [15].

3.3.2. First order scheme. To summarize, we write down the following first order scheme for the heavy tail case. The spatial derivative is treated using the Fourier transform based spectral method. Letting k be the variable as opposed to x, we denote variables with a hat as their corresponding quantities in the Fourier space:

(3.40)
$$\begin{cases} \epsilon^\alpha \dfrac{\hat\rho^{n+1}-\hat\rho^n}{\Delta t} = \left\langle \nu_B^{\mathbf{t}} \hat g_B^{n+1}\right\rangle + \left\langle \nu_T^{\mathbf{t}} \hat g_T^{n+1}\right\rangle, \\ \epsilon^\alpha \dfrac{\hat g_B^{n+1}-\hat g_B^n}{\Delta t} + i\epsilon v\cdot k(\hat\rho^* \mathcal{M}_B + \hat g_B^{n+1}) \\ \qquad = -\nu_B^{\mathbf{t}} \hat g_B^{n+1} + \displaystyle\int \phi(v_B, v_B')\hat g_B^{n\prime}\,\mathrm{d}v' \mathcal{M}_B^{\mathbf{t}} - \iint \phi(v_B, v_B')\hat g_B^{n\prime}\,\mathrm{d}v' \mathcal{M}_B^{\mathbf{t}} dv \dfrac{\mathcal{M}_B^{\mathbf{t}}}{\left\langle \mathcal{M}_B^{\mathbf{t}}\right\rangle}, \\ \dfrac{1}{\epsilon^\alpha}\left\langle \nu_T^{\mathbf{t}} \hat g_T^{n+1}\right\rangle = -\dfrac{1}{\epsilon^\alpha}\displaystyle\int_{|v|\ge v_{\max}} \frac{i\epsilon v\cdot k \nu_T^{\mathbf{t}}}{\nu_T^{\mathbf{t}} + i\epsilon v\cdot k}\mathcal{M}_T^{\mathbf{t}}(v)\,\mathrm{d}v \hat\rho^*, \end{cases}$$

where $\hat\rho^*$ can again be chosen as $\hat\rho^n$ or $\hat\rho^{n+1}$.

To be more precise, we list out the steps needed in our scheme. First choose $v_{\max}$ such that it meets the criteria (3.39). Denote

$$C_\epsilon(k) = \frac{1}{\epsilon^\alpha}\int_{|v|\ge v_{\max}} \frac{\nu_T^{\mathbf{t}}\left(\epsilon v\cdot k\right)^2}{{\nu_T^{\mathbf{t}}}^2 + \left(\epsilon v\cdot k\right)^2}\mathcal{M}_T^{\mathbf{t}}(v)\,\mathrm{d}v, \tag{3.41}$$

and precompute it with a prescribed accuracy. Then given $\left\langle \nu_T^{\mathbf{t}} \hat g_T^n\right\rangle(k)$, $\hat g_B^n(k,v)$, and $\hat\rho^n(k)$, we have the following, at time t^{n+1}:

- Step 1. Compute $\frac{1}{\epsilon^\alpha}\left\langle \nu_T^{\mathbf{t}} \hat g_T^{n+1}(k,v)\right\rangle$ via

$$\frac{1}{\epsilon^\alpha}\left\langle \nu_T^{\mathbf{t}} \hat g_T^{n+1}(k,v)\right\rangle = -C_\epsilon(k)\hat\rho^*(k). \tag{3.42}$$

  If $\rho^* = \rho^n$, one can get the values for $\left\langle \nu_T^{\mathbf{t}} \hat g_T^{n+1}\right\rangle(k)$. If $\rho^* = \rho^{n+1}$, one writes $\left\langle \nu_T^{\mathbf{t}} \hat g_T^{n+1}\right\rangle(k)$ in terms of $\hat\rho^{n+1}(k)$.
- Step 2. Solve $\hat g_B^{n+1}(k,v)$ for $|v|\le v_{\max}$ from the second equation in (3.40). Again if $\hat\rho^* = \hat\rho^n$, one can get the values for $\hat g_B^{n+1}$; and if $\hat\rho^* = \hat\rho^{n+1}$, one writes $\hat g_B^{n+1}(k)$ in terms of $\hat\rho^{n+1}(k)$.
- Step 3. Compute $\left\langle \nu_B^{\mathbf{t}} \hat g_B^{n+1}\right\rangle$ by a simple quadrature rule of $\nu_B^{\mathbf{t}} \hat g_B^{n+1}$ in velocity space.
- Step 4. Plug $\frac{1}{\epsilon^\alpha}\left\langle \nu_B^{\mathbf{t}} \hat g_B^{n+1}\right\rangle$ and $\frac{1}{\epsilon^\alpha}\left\langle \nu_T^{\mathbf{t}} \hat g_T^{n+1}\right\rangle$ into

$$\hat\rho^{n+1} = \hat\rho^n + \frac{\Delta t}{\epsilon^\alpha}\left(\left\langle \nu_T^{\mathbf{t}} \hat g_T^{n+1}\right\rangle + \left\langle \nu_B^{\mathbf{t}} \hat g_B^{n+1}\right\rangle\right)$$

  to get $\hat\rho^{n+1}(k)$.

Repeat the above three steps until the end of time $t = t^M$, and perform the inverse Fourier transform to get $\rho^M(x)$ and $g_B^M(x,v)$ from $\hat\rho^M(k)$ and $\hat g_B^M(k,v)$, respectively, and recover $f^M(x,v)$ via

$$f^M(k,v) = \rho^M(x)\frac{\mathcal{M}_B^{\mathbf{t}}(v)}{\left\langle \mathcal{M}_B^{\mathbf{t}}(v)\right\rangle} + g_B^M(x,v) \qquad \text{for } |v|\le v_{\max}. \tag{3.43}$$

3.4. Numerical scheme: Degenerate collision frequency.

3.4.1. Velocity discretization. In contrast with the heavy tail case, the equilibrium $\mathcal{M}^{\mathbf{d}}$ has a compact support and there is no special care needed in the truncation of the velocity space. Rather, it is the small velocity that makes the major contribution when ϵ is small, as seen in the integral (2.14) in Lemma 2.3. Therefore, to capture the correct asymptotic limit numerically, we need to calculate this integration accurately enough around the origin, which, as a result, requires finer mesh for smaller ϵ. Then the question immediately arises: finer mesh in the velocity space needs more expensive computation. However, this integration is independent of time and thus can be precomputed with arbitrary accuracy.

To be more precise, recall the semidiscrete scheme (3.11), then upon the Fourier transform in space, it reads

$$\frac{\hat{\rho}^{n+1}-\hat{\rho}^n}{\Delta t}=\frac{1}{\epsilon^\alpha}\left\langle \mathcal{K}(\hat{g}^{n+1})\right\rangle=\frac{1}{\epsilon^\alpha}\left\langle \nu^{\mathbf{d}}\hat{g}^{n+1}\right\rangle, \tag{3.44}$$

$$\frac{\epsilon^\alpha}{\Delta t}(\hat{g}^{n+1}-\hat{g}^n)+i\epsilon v\cdot k(\hat{\rho}^*\mathcal{M}^{\mathbf{d}}+\hat{g}^{n+1})=-\nu^{\mathbf{d}}\hat{g}^{n+1}+\mathcal{K}(\hat{g}^n)-\left\langle \mathcal{K}(\hat{g}^n)\right\rangle\mathcal{M}^{\mathbf{d}}, \tag{3.45}$$

where (3.45) implies

$$\hat{g}^{n+1}=-\frac{i\epsilon v\cdot k\mathcal{M}^{\mathbf{d}}}{\frac{\epsilon^\alpha}{\Delta t}+\nu^{\mathbf{d}}+i\epsilon v\cdot k}\hat{\rho}^*+\frac{\frac{\epsilon^\alpha}{\Delta t}\hat{g}^n+\mathcal{K}(\hat{g}^n)-\left\langle \mathcal{K}(\hat{g}^n)\right\rangle\mathcal{M}^{\mathbf{d}}}{\frac{\epsilon^\alpha}{\Delta t}+\nu^{\mathbf{d}}+i\epsilon v\cdot k}.$$

Hence

$$\frac{1}{\epsilon^\alpha}\left\langle \nu^{\mathbf{d}}\hat{g}^{n+1}\right\rangle=-\frac{1}{\epsilon^\alpha}\left\langle \frac{i\epsilon v\cdot k\mathcal{M}^{\mathbf{d}}\nu^{\mathbf{d}}}{\frac{\epsilon^\alpha}{\Delta t}+\nu^{\mathbf{d}}+i\epsilon v\cdot k}\right\rangle\hat{\rho}^*+\frac{1}{\epsilon^\alpha}\left\langle \nu^{\mathbf{d}}\frac{\frac{\epsilon^\alpha}{\Delta t}\hat{g}^n+\mathcal{K}(\hat{g}^n)-\left\langle \mathcal{K}(\hat{g}^n)\right\rangle\mathcal{M}^{\mathbf{d}}}{\frac{\epsilon^\alpha}{\Delta t}+\nu^{\mathbf{d}}+i\epsilon v\cdot k}\right\rangle. \tag{3.46}$$

Then our idea is to compute the first integral on the right-hand side of (3.46) accurately. This is accomplished as follows. Like what is done analytically (see the proof in Lemma 2.3), let

$$w=\frac{\epsilon|k|v}{\nu_0|v|^{\gamma+1}},\quad \mathrm{d}v=\frac{1}{\gamma}\left(\frac{\epsilon|k|}{\nu_0|w|^{\gamma+1}}\right)^{\frac{N}{\gamma}}\mathrm{d}w, \tag{3.47}$$

and recalling (1.15), we have

$$\begin{aligned}\mathcal{BODY}(\epsilon,k)&:=\frac{1}{\epsilon^\alpha}\left\langle \frac{i\epsilon v\cdot k\mathcal{M}^{\mathbf{d}}\nu^{\mathbf{d}}}{\frac{\epsilon^\alpha}{\Delta t}+\nu^{\mathbf{d}}+i\epsilon v\cdot k}\right\rangle=\frac{1}{\epsilon^\alpha}\int_{|v|\le\delta}\frac{(\epsilon v\cdot k)^2\mathcal{M}_0\nu_0|v|^{\gamma+1}}{\left(\frac{\epsilon^\alpha}{\Delta t}+\nu^{\mathbf{d}}\right)^2+(\epsilon v\cdot k)^2}\mathrm{d}v\\&=\frac{1}{\epsilon^\alpha}\int_{|w|\ge\frac{\epsilon|k|}{\nu_0\delta^\gamma}}\frac{\mathcal{M}_0(w\cdot e)^2\nu_0\left(\frac{\epsilon|k|}{\nu_0|\omega|}\right)^{\frac{\gamma+1}{\gamma}}}{\left[\frac{\epsilon^\alpha}{\Delta t\nu_0}\left(\frac{\nu_0|w|}{\epsilon|k|}\right)^{\frac{\gamma+1}{\gamma}}+1\right]^2+(w\cdot e)^2}\left(\frac{\epsilon|k|}{\nu_0|w|^{\gamma+1}}\right)^{\frac{N}{\gamma}}\frac{1}{\gamma}\mathrm{d}w\\&=|k|^\alpha\frac{\mathcal{M}_0\nu_0^{1-\alpha}}{\gamma}\int_{|w|\ge\frac{\epsilon|k|}{\nu_0\delta^\gamma}}\frac{(w\cdot e)^2}{(w\cdot e)^2+\left[1+\frac{\nu_0^{\frac{1}{\gamma}}}{\Delta t}\left(\frac{|w|}{|k|}\right)^{\frac{\gamma+1}{\gamma}}\epsilon^{\frac{N}{\gamma}}\right]^2}\frac{1}{|w|^{\frac{(N+1)(\gamma+1)}{\gamma}}}\mathrm{d}w,\end{aligned} \tag{3.48}$$

where the singularity in the last integral can be treated using integration by parts.

Here e is an unitary vector. Once $\mathcal{BODY}$ is computed, (3.46) reduces to

$$\frac{1}{\epsilon^\alpha}\left\langle \nu^{\mathbf{d}}\hat{g}^{n+1}\right\rangle = -\mathcal{BODY}\hat{\rho}^* + \frac{1}{\epsilon^\alpha}\left\langle \nu^{\mathbf{d}}\frac{\frac{\epsilon^\alpha}{\Delta t}\hat{g}^n + \mathcal{K}(\hat{g}^n) - \langle \mathcal{K}(\hat{g}^n)\rangle \mathcal{M}^{\mathbf{d}}}{\frac{\epsilon^\alpha}{\Delta t} + \nu^{\mathbf{d}} + i\epsilon v\cdot k}\right\rangle,$$

and we can summarize the first order scheme in the next subsection.

We would like to make a remark on the difference of our scheme here as compared to what is designed in [9]. Aside from the similarity in dealing with the singularity at the origin through a change of variable, the main ideas are completely different. More specifically, we single out the role of the body, which can be considered as the counterpart of the tail in the previous case. As the tail and body constitute the major component in the fractional diffusion in these two scenarios, the same idea —precomputing the main part—applies in both cases.

3.4.2. First order scheme. Simply put, the first order scheme for the degenerate collision frequency case reads

$$\begin{cases} \dfrac{\hat{\rho}^{n+1}-\hat{\rho}^n}{\Delta t} = -\mathcal{BODY}\hat{\rho}^* + \dfrac{1}{\epsilon^\alpha}\left\langle \nu^{\mathbf{d}}\dfrac{\frac{\epsilon^\alpha}{\Delta t}\hat{g}^n + \mathcal{K}(\hat{g}^n) - \langle \mathcal{K}(\hat{g}^n)\rangle \mathcal{M}^{\mathbf{d}}}{\frac{\epsilon^\alpha}{\Delta t} + \nu^{\mathbf{d}} + i\epsilon v\cdot k}\right\rangle, \\ \hat{g}^{n+1} = -\dfrac{i\epsilon v\cdot k\mathcal{M}^{\mathbf{d}}}{\frac{\epsilon^\alpha}{\Delta t} + \nu^{\mathbf{d}} + i\epsilon v\cdot k}\hat{\rho}^* + \dfrac{\frac{\epsilon^\alpha}{\Delta t}\hat{g}^n + \mathcal{K}(\hat{g}^n) - \langle \mathcal{K}(\hat{g}^n)\rangle \mathcal{M}^{\mathbf{d}}}{\frac{\epsilon^\alpha}{\Delta t} + \nu^{\mathbf{d}} + i\epsilon v\cdot k}, \end{cases} \tag{3.49}$$

where $\hat{\rho}^*$ can be either $\hat{\rho}^n$ or $\hat{\rho}^{n+1}$. A more detailed algorithm is summarized as follows. Before starting the time evolution, we first compute $\mathcal{BODY}$ in (3.48) with a very fine mesh in v. Here the singularity is treated using integration by parts, the infinite domain is replaced by a big enough computational domain via trial and error. And we store the values of $\mathcal{BODY}$ for different k in a table. Then given $\hat{\rho}^n(k)$ and $\hat{g}^n(k,v)$, we have the following, at time t^{n+1}:

- Step 1. Compute $\hat{\rho}^{n+1}$ from the first equation in (3.49). If $\hat{\rho}^* = \hat{\rho}^{n+1}$, this equation can be easily inverted.
- Step 2. Compute $\hat{g}^{n+1}$ through the second equation in (3.49).

Repeat the above three steps until the end of time $t = t^M$, and f^M is restored from

$$f^M(x,v) = \rho^M(x)\mathcal{M}^{\mathbf{d}}(v) + g^M(x,v) \qquad \text{for } |v|\le\delta \tag{3.50}$$

with $\rho^M(x)$ and $g^M(x,v)$ obtained from the inverse Fourier transform.

Two remarks are in order.

Remark 3.6.

(1) The scheme we designed here can be directly generalized to the spatial dependent collision, as was done in [24].

(2) A second order scheme can be constructed for (3.40) and (3.49) using the backward difference formula. Specifically, one can just replace the time discretization by $\frac{3\rho^{n+1}-4\rho^n+\rho^{n+1}}{2\Delta t}$, and replace any term at t^n by an extrapolation. See [24] for more details.

4. Numerical examples. This section is devoted to numerical illustration of our AP schemes for the anisotropic transport equation in both kinetic and fractional diffusion regimes. Here the spatial domain is chosen $x\in[0,2\pi]$ with periodic boundary condition, and the derivative in x is treated via the Fourier spectral method. Without further notice, we use the implicit method, meaning that $\rho^* = \rho^{n+1}$ in the schemes.

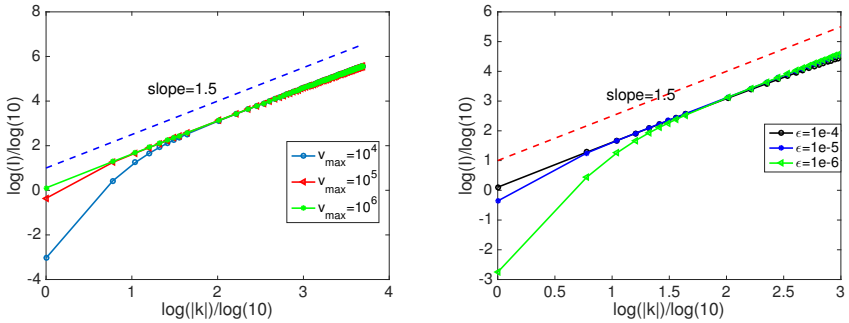

FIG. 4.1. *Plot of* $\log(I)/\log(10)$ *versus* $\log(|k|)/\log(10)$. $\alpha = 1.5$. *Left:* $\epsilon = 10^{-5}$, *varying cutoff* v_{max}. *Right:* $v_{max} = 10^5$, *varying* ϵ. *Here the number of velocity points is* $20 \times v_{max}$.

For the heavy tail case, we choose

$$\phi^{\mathbf{t}}(v,v') = 1 + e^{-v^2-v'^2}, \quad \mathcal{M}^{\mathbf{t}}(v) = \begin{cases} \frac{\alpha}{2+2\alpha}\frac{1}{|v|^{1+\alpha}} & \text{for } |v| \geq 1, \\ \frac{\alpha}{2+2\alpha} & \text{for } 0 \leq |v| < 1; \end{cases} \tag{4.1}$$

and for the degenerate collision frequency case, we use

$$\mathcal{M}^{\mathbf{d}}(v) = \begin{cases} \frac{1}{2} & \text{for } 0 \leq |v| \leq 1, \\ 0 & \text{for } |v| > 1, \end{cases} \quad \nu(v) = \nu_0|v|^{1+\gamma}, \quad \phi(v,v') = \frac{\nu(v)\nu(v')}{\langle \nu \mathcal{M}^{\mathbf{d}} \rangle}, \tag{4.2}$$

where

$$\gamma = \beta + 2, \quad \alpha = \frac{\beta+4}{\beta+2}, \quad \beta > 0. \tag{4.3}$$

ν_0 is chosen such that $\sum_j \nu(v_j)\mathcal{M}^{\mathbf{d}}(v_j)\Delta v = 1$ only to simplify the computation of $\phi(v,v')$ in (4.2).

4.1. Tail effect. In the first test, we will address the need of adding the tail in the heavy tail equilibrium case. Particularly, we compute the following integral in the truncated velocity space $\{|v| < v_{\max}\}$,

$$I(k) = \frac{1}{\epsilon^\alpha} \int_{|v|<v_{\max}} \frac{(\epsilon v k)^2}{{\nu^{\mathbf{t}}}^2 + (\epsilon v k)^2} \nu^{\mathbf{t}}(v)\mathcal{M}^{\mathbf{t}}(v)\,\mathrm{d}v \tag{4.4}$$

which arises in (3.22) and constitutes a major part in the diffusion limit. Here $\mathcal{M}^{\mathbf{t}}$ takes the form in (4.1) and

$$\nu^{\mathbf{t}}(v) = \int_{|v|<v_{\max}} \phi^{\mathbf{t}}(v,v')\mathcal{M}^{\mathbf{t}}(v')\,\mathrm{d}v.$$

With a varying $v_{\max}$, Figure 4.1 on the left displays $I(k)$ in terms of k for $\alpha = 1.5$ and $\epsilon = 10^{-5}$. On the right of Figure 4.1, we show the change of $I(k)$ with a fixed $v_{\max} = 10^5$ but varying ϵ. As shown, $v_{\max}$ has to be large enough such that $I(k)$ behaves like $|k|^\alpha$ for all ranges of k, and $v_{\max}$ increases with vanishing ϵ.

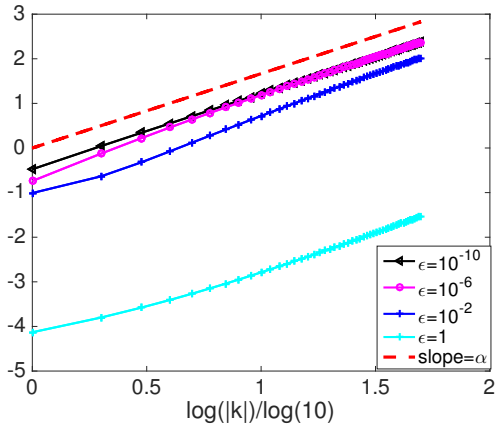

FIG. 4.2. *Plot of* $\log(I_2)/\log(10)$ *versus* $\log(|k|)/\log(10)$ *for different* ϵ. *Here* $\beta = 1$, *and* $\alpha = 5/3$, $\Delta t = 0.02$. *The number of velocity points is* 10^6.

4.2. Velocity discretization effect for degenerate collision frequency case. For the degenerate case, we check that the computation of the body part gives us the correct behavior when ϵ is small. In one dimension, (3.48) reduces to

$$
\begin{aligned}
I_2(k,\epsilon) &= \frac{1}{\epsilon^\alpha}\int_{|v|\le 1} \frac{i\epsilon v\cdot k\nu\mathcal{M}^{\mathbf{d}}}{\frac{\epsilon^\alpha}{\Delta t}+\nu^{\mathbf{d}}+i\epsilon v\cdot k}\,\mathrm{d}v \\
&= |k|^\alpha \frac{\mathcal{M}_0\nu_0^{1-\alpha}}{\gamma}\frac{2}{2-\alpha}\left[-\frac{(\frac{\epsilon|k|}{\nu_0})^{2-\alpha}}{\left(\frac{\epsilon|k|}{\nu_0}\right)^2+\left(1+a\left|\frac{w}{k}\right|^{\frac{\gamma+1}{\gamma}}\right)^2}\right. \\
&\quad \left. +\int_{\frac{\epsilon|k|}{\nu_0}}^{+\infty}\frac{w^{2-\alpha}\left(2w+2\left(1+a\left|\frac{w}{k}\right|^{\xi}\right)\frac{a}{|k|^\xi}\xi w^{\xi-1}\right)}{\left[w^2+\left(1+\left|\frac{w}{k}\right|^{\frac{\gamma+1}{\gamma}}a\right)^2\right]^2}\,\mathrm{d}w\right],
\end{aligned}
\tag{4.5}
$$

where $a = \epsilon^{\frac{N}{\gamma}}\frac{\nu_0^{\frac{1}{\gamma}}}{\Delta t}$ and $\xi = \frac{\gamma+1}{\gamma}$. Figure 4.2 plots $I_2(k)$ for different ϵ's in log scale. It is obvious that when ϵ is getting smaller, $\log(I_2(k))$ has the shape of a straight line in terms of $\log(|k|)$ with a slope α, indicating that $I_2(k)\propto|k|^\alpha$ for small ϵ, a key element in preserving the asymptotic limit for (3.49).

4.3. Test on asymptotic property. In the course of showing the asymptotic property in section 3.2, the quantity $\langle\nu g\rangle$ plays a key role. Therefore, we consider $\int|\langle\nu g\rangle|dx$ as the indicator for the asymptotic error, which, in the discrete version, is written

$$
E_{\langle\nu g\rangle} = \sum_i\Big|\sum_j \nu_j g_{i,j}\Big|\Delta x\Delta v\,,\quad \nu_j=\nu(v_j)\,,\ g_{i,j}\simeq g(x_i,v_j)\,.
\tag{4.6}
$$

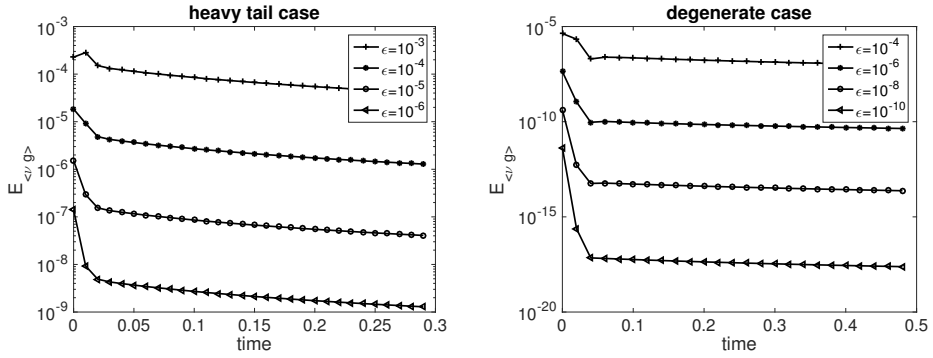

FIG. 4.3. *Left: heavy tail equilibrium case. Plot of* (4.6) *versus time.* $\Delta t = 0.01$, $\Delta x = 0.0628$, $v_{max} = 100$, $\Delta v = 0.078$, $\alpha = 1.5$. *Right: Degenerate collision case. Plot of* (4.7) *versus time.* $\Delta t = 0.02$, $\Delta x = 0.0314$, $v_{max} = 1$, $\Delta v = 0.0078$, $\alpha = 5/3$.

Special care needs to be taken for the heavy tail case, and we have a modified version of (4.6):

$$E_{\langle \nu g \rangle} = \sum_i \Big| \sum_j \nu_j g_{i,j} + \langle \nu_T g_T \rangle_i \Big| \Delta x \Delta v \,, \tag{4.7}$$

where $\langle \nu_T g_T \rangle$ is computed via (3.38).

For the heavy tail case, the initial data are chosen as

$$f(0,x,v) = \frac{1}{\sqrt{\pi}} e^{-v^2} e^{-5(x-\pi)^2}, \quad x \in [0, 2\pi] \,, \tag{4.8}$$

with a velocity cutoff $v_{\max} = 100$ and meshes $\Delta x = 0.0628$, $\Delta v = 0.0781$, $\Delta t = 0.01$, whereas for the degenerate case, the initial data are chosen the same but with a different computational domain for v, i.e.,

$$f(0,x,v) = \frac{1}{\sqrt{\pi}} e^{-v^2} e^{-5(x-\pi)^2}, \quad x \in [0, 2\pi], \quad v \in [-1, 1] \,. \tag{4.9}$$

The results are collected in Figure 4.3. It is seen that for both cases, we have $E_{\langle \nu g \rangle} = \mathcal{O}(\epsilon)$ at the beginning of the simulation. This is the result of the initial splitting in (3.5). Then $E_{\langle \nu g \rangle}$ decays to $\mathcal{O}(\epsilon^\alpha)$ with $\alpha = 1.5$ and $\alpha = \frac{5}{3}$, respectively, suggesting the AP property of our scheme on both models, as proved in section 3.2.

In addition, since g represents the the microscopic component, we also check the energy of g,

$$E_g = \sum_{i,j} \frac{g_{i,j}^2}{\mathcal{M}_{i,j}} \Delta x \Delta v \tag{4.10}$$

with varying ϵ and collect the results in Figure 4.4. Here in both cases, an obvious decrease of such an energy with respect to the decrease of ϵ is observed.

4.4. Stability test. We now check the dissipation of total energy (3.6) and boundedness of energy for g and ρ in (3.9), respectively. Numerically, the energy is computed via a simple summation

$$E_f = \sqrt{\sum_i \sum_j \frac{(\rho_i \mathcal{M}_j + g_{i,j})^2}{\mathcal{M}_j} \Delta x \Delta v}, \quad E_\rho = \sqrt{\sum_i \rho_i^2 \Delta x}, \quad E_g = \sqrt{\sum_i \frac{g_{i,j}}{\mathcal{M}_j} \Delta x \Delta v}. \tag{4.11}$$

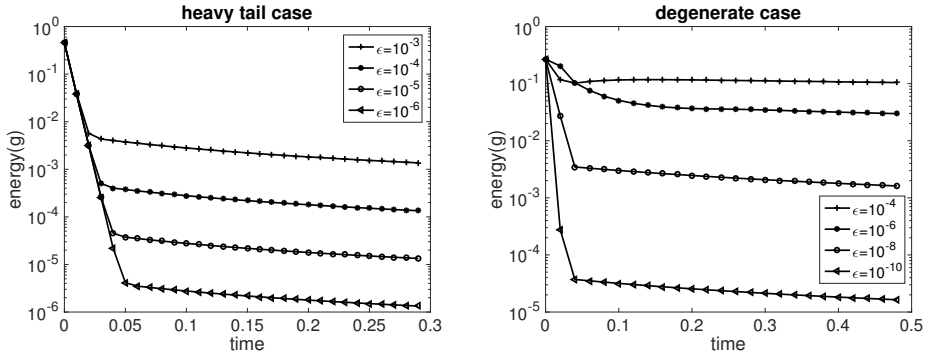

FIG. 4.4. *Plot of energy g* (4.10) *versus time. Left: fat tail case.* $\Delta t = 0.01$, $\Delta x = 0.0628$, $v_{max} = 100$, $\Delta v = 0.078$, $\alpha = 1.5$. *Right: degenerate collision case.* $\Delta t = 0.02$, $\Delta x = 0.0314$, $v_{max} = 1$, $\Delta v = 0.0078$, $\alpha = 5/3$.

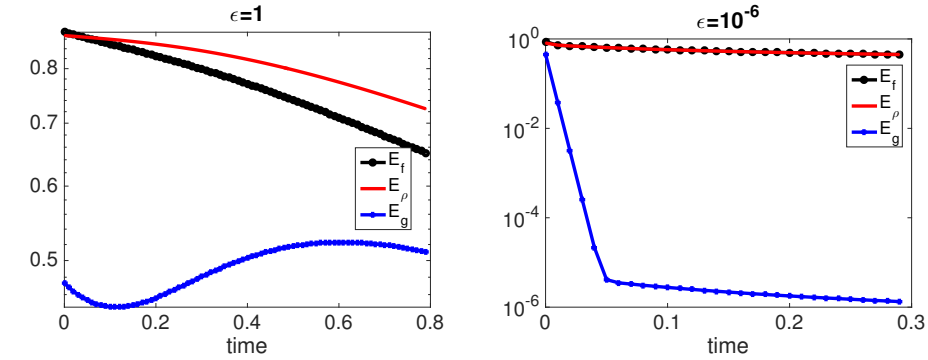

FIG. 4.5. *Plot of energy in f, ρ, and g in* (4.11) *versus time for the heavy tail case.* $\Delta t = 0.01$, $\Delta x = 0.0628$, $v_{max} = 100$, $\alpha = 1.5$ *in* (1.12). *Left:* $\epsilon = 1$. *Right:* $\epsilon = 10^{-6}$.

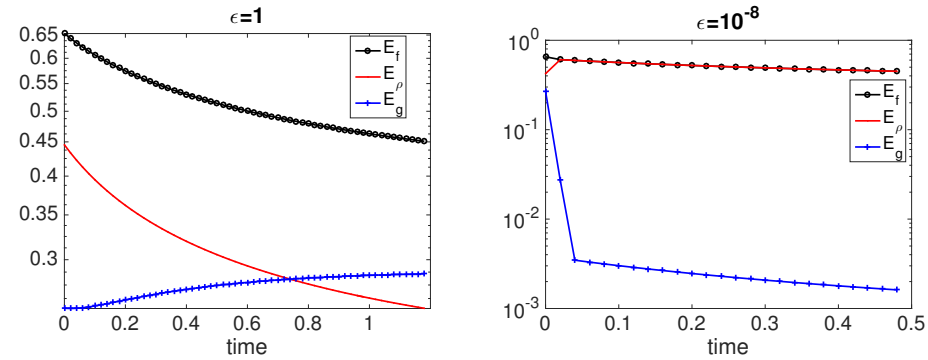

FIG. 4.6. *Plot of energy in f, ρ, and g* (4.11) *versus time for the degenerate collision frequency case.* $\Delta t = 0.02$, $\Delta x = 0.0628$, $v_{max} = 1$, $\alpha = \frac{5}{3}$ *in* (1.12). *Left:* $\epsilon = 1$. *Right:* $\epsilon = 10^{-8}$.

Here we use the same setup as in section 4.3 for both cases and we plot the energy for $\epsilon = 1$, and $\epsilon = 10^{-6}$ for the heavy tail case and $\epsilon = 1$ and 10^{-8} for the degenerate collision frequency case. The results are collected in Figure 4.5 for the fat tail equilibrium case and Figure 4.6 for the degenerate collision frequency case. As expected

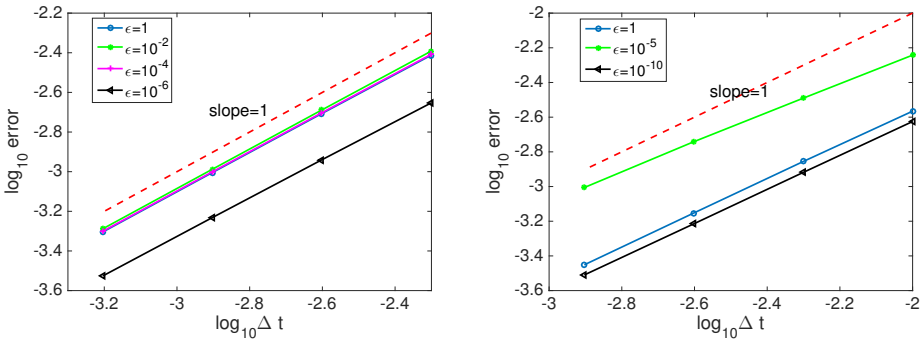

FIG. 4.7. *Convergence test for the first order scheme. Left: fat tail case with scheme* (3.40). *Right: degenerate case with scheme* (3.49).

in section 3.1, the total energy E_f decays with time, and the energies for ρ and g are uniformly bounded.

4.5. Convergence test. The test in this section is devoted to checking the first order convergence of our scheme (3.40) and (3.49) in time for both scenarios. For the heavy tail case, the initial condition is the same as (4.8), and the simulation is performed up to time $T = 0.2$, with number of time steps $N_t = 20, 40, 80, 160, 320$. $v_{\max}$ is taken to be 100, and we choose $\alpha = 1.5$, $N_x = 100$, and $N_v = 2560$. For the degenerate case, the initial condition takes (4.9), and final time is $T = 0.4$ with the same partition of time steps from 20 to 320, increased twice each time. Here $\beta = 1$, $N_x = 200$, $N_v = 800$. The error is computed via

$$\text{error}_{\Delta t} = \|f_{\Delta t} - f_{\Delta t/2}\|_1 = \sum_{i,j} |(f_{\Delta t}(T))_{i,j} - (f_{\Delta t/2}(T))_{i,j}| \Delta x \Delta v \,.$$

In Figure 4.7 the implicit first order method is tested and expected first order convergence is observed.

4.6. Nonsmooth initial data. In this test, we consider nonsmooth initial data

$$f(0, x, v) = \frac{1}{\sqrt{\pi}} e^{-v^2} \mathbf{1}_{|x-\pi| \le 0.5} \tag{4.12}$$

with $x \in [0, 2\pi]$ and $v \in [-1, 1]$ for the degenerate case and $v \in [-100, 100]$ for the heavy tail case. First, we compare the solution to our AP scheme with the explicit solver to the original equation (1.7) for $\epsilon = 1$ and with the diffusion solver for the limiting equation (2.12) or (2.20) when ϵ is small. The results in the density ρ are gathered in Figures 4.8 and 4.9 for two cases, at output time $t = 0.3$ and $t = 0.5$, respectively. In both cases, good agreement is observed, indicating the effectiveness of our scheme in both kinetic and fractional diffusion regimes. Here we would like to mention that for the degenerate collision case we choose $\epsilon = 10^{-6}$ because the convergence to equilibrium is rather slow, the asymptotic error of which is around $\mathcal{O}\left(\epsilon^{\frac{N}{N+1+\beta}}\right) + \mathcal{O}\left(\epsilon^{\frac{\beta}{N+1+\beta}}\right)$, as explained in [9].

4.7. Different α. Here we take the same setup as in section 4.6 but with varying α. In Figure 4.10, the profile of ρ is displayed for $\alpha = 1.2$, 1.5, and 1.8 for the heavy tail case at $t = 0.3$. When $\epsilon = 10^{-5}$, larger α leads to stronger diffusion, as one

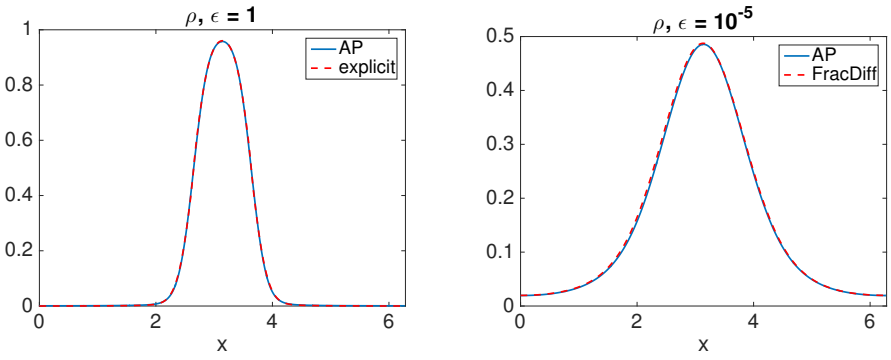

FIG. 4.8. *Plot of ρ for the heavy tail case at time $t = 0.3$ with initial data* (4.12). $\Delta x = 0.0157$, $\alpha = 1.5$. *Left:* $\epsilon = 1$. *Right:* $\epsilon = 10^{-5}$.

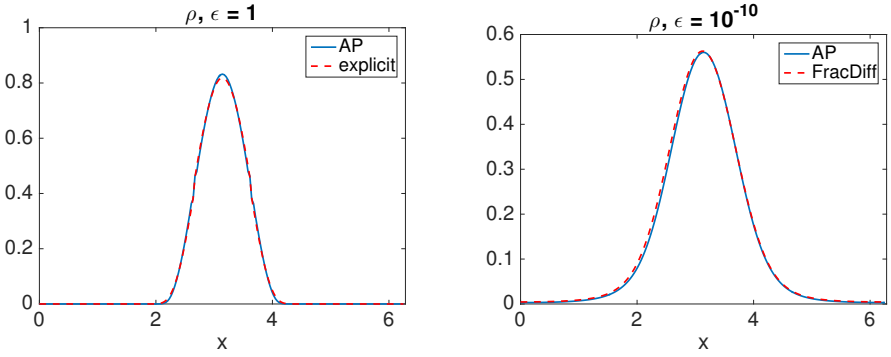

FIG. 4.9. *Plot of ρ for the degenerate collision frequency case at time $t = 0.5$ with initial data* (4.12). $\Delta x = 0.0314$, $\alpha = \frac{5}{3}$, $\Delta t = 0.02$. *Left:* $\epsilon = 1$. *Right:* $\epsilon = 10^{-10}$.

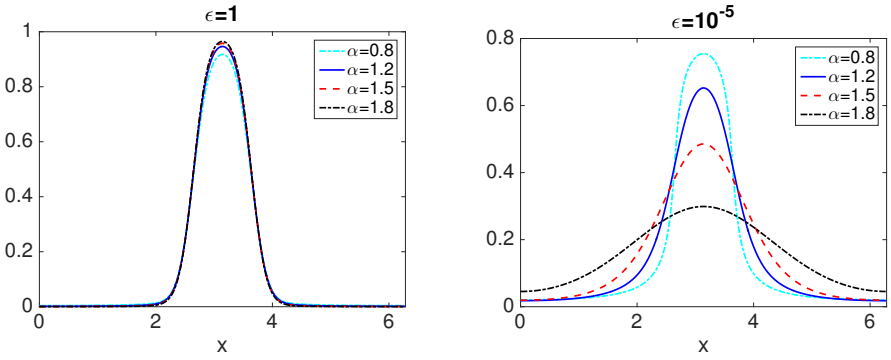

FIG. 4.10. *Plot of ρ for the heavy tail case at time $t = 0.3$ for different α. Initial data are chosen as* (4.12). $\Delta x = 0.0157$, $\Delta t = 0.01$. *Left:* $\epsilon = 1$. *Right:* $\epsilon = 10^{-5}$.

would expect from the limiting equation (2.12). In contrast, the solution does not vary too much for $\epsilon = 1$, and an opposite trend is observed—smaller α induces larger "diffusion." Similar observation can be made for the degenerate collision frequency case, whose result is summarized in Figure 4.11.

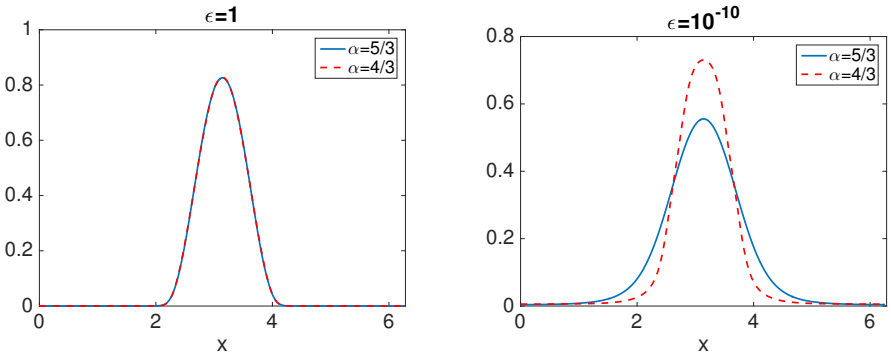

FIG. 4.11. *Plot of ρ for the degenerate collision frequency case at time $t = 0.5$ for different α. Initial data are chosen as* (4.12). $\Delta x = 0.0314$, $\Delta t = 0.02$. *Left:* $\epsilon = 1$. *Right:* $\epsilon = 10^{-10}$.

5. Conclusion. We constructed an AP scheme for a linear kinetic equation with anisotropic scattering, whose asymptotic limit is a fractional diffusion equation. This limit emerges due to the unboundedness of the diffusion matrix in the classical diffusion limit and it is attributed to two different reasons. One is the heavy tail equilibrium and the other is the degenerate collision frequency. We consider both cases here. Our idea follows that in [24], but with three major contributions: (1) we provide a special treatment of the anisotropy for the collision cross section, which results in a different macro-micro splitting of the original equation; (2) we showed, via detailed calculation, the relaxed asymptotic property owing to the two extra terms coming from the anisotropic scattering. We also mention a direction that can accelerate the convergence; (3) for the degenerate collision frequency case that has not been considered before, we introduce a precomputation of integrated body rather than an integrated tail in the other scenario, and it is implemented through a change of variable. Numerical examples are carried out in the end to validate the needs of adding the tail or computing the body, the asymptotic property, and the effectiveness.

6. Appendix.

Proof of Proposition 3.4. To lighten the notation, we omit the superscript n when it dose not cause any confusion in this appendix. First we cite the following formula that will be used throughout the proof. For any vectors v, $k \in \mathbf{R}^N$, we have

$$\begin{aligned}
&\int_{|v|\le\delta} f(v\cdot k)dv \\
&= \int_0^\delta \int_0^\pi \cdots \int_0^\pi \int_0^{2\pi} f(r|k|\cos\theta) r^{N-1} \sin^{N-2}\theta \sin^{N_3}\phi_1 \cdots \sin^{\phi_{N-3}} \mathrm{d}r\,\mathrm{d}\theta\,\mathrm{d}\phi_1 \cdots \mathrm{d}\phi_{N-2} \\
&:= \int_0^\delta \int_{\mathcal{S}} f(r|k|\cos\theta) r^{N-1}\,\mathrm{d}r\,\mathrm{d}\,\mathbf{s}\,.
\end{aligned}$$

(1) Notice from the definition of $\mathcal{A}$ and $\mathcal{B}$ in (3.14) that

$$|\mathcal{A}| \le M_0\,, \quad |\mathcal{B}| \le 1\,. \tag{6.1}$$

Also, the third term $\mathcal{C}\hat{g}^n$ is bounded in the special case (3.16). Indeed, from

(3.13), we have

$$\left\langle -\nu^{\mathbf{d}}\hat{g}^{n+1}\right\rangle = \left\langle \epsilon^{\alpha}\frac{\hat{g}^{n+1}-\hat{g}^{n}}{\Delta t} + i\epsilon v\cdot k\hat{g}^{n+1}\right\rangle \tag{6.2}$$

and, thus,

$$|\mathcal{C}\hat{g}^{n+1}| = \left|\frac{\nu^{\mathbf{d}}\mathcal{M}^{\mathbf{d}}}{\langle\nu^{\mathbf{d}}\mathcal{M}^{\mathbf{d}}\rangle} - \mathcal{M}^{\mathbf{d}}\right| \left|\frac{\left\langle \epsilon^{\alpha}\frac{\hat{g}^{n+1}-\hat{g}^{n}}{\Delta t} + i\epsilon v\cdot k\hat{g}^{n+1}\right\rangle}{\frac{\epsilon^{\alpha}}{\Delta t}+\nu^{\mathbf{d}}+i\epsilon v\cdot k}\right| \lesssim \mathcal{O}(1)|\hat{g}^{n+1}|\,. \tag{6.3}$$

Therefore, if initially $\hat{\rho}$ and $\hat{g}$ are bounded, then $\hat{g}$ obtained by (3.13) is bounded.

(2) We first look at the term $\mathcal{B}\mathcal{A}\hat{\rho}$. Recall that $\nu^{\mathbf{d}} = \nu_0|v|^{1+\gamma}$, for $|v|\le\delta$ we have

$$\begin{aligned}
\left|\frac{1}{\epsilon^{\alpha}}\left\langle\mathcal{K}(\mathcal{B}\mathcal{A}\hat{\rho})\right\rangle\right| &= \left|\frac{1}{\epsilon^{\alpha}}\left\langle\nu^{\mathbf{d}}\mathcal{B}\mathcal{A}\hat{\rho}\right\rangle\right| = \left|\int_{|v|\le\delta}\nu^{\mathbf{d}}\frac{i\epsilon|v\cdot k|}{\left(\frac{\epsilon^{\alpha}}{\Delta t}+\nu^{\mathbf{d}}+i\epsilon v\cdot k\right)^2}\,\mathrm{d}v\hat{\rho}\frac{M_0}{\Delta t}\right| \\
&\lesssim \int_0^{\delta}\int_{\mathcal{S}}\frac{\nu^{\mathbf{d}}\epsilon r|k|\cos\theta r^{N-1}}{\left(\frac{\epsilon^{\alpha}}{\Delta t}+\nu^{\mathbf{d}}\right)^2+(\epsilon r|k|\cos\theta)^2}\,\mathrm{d}r\,\mathrm{d}\mathbf{s} \qquad (6.4)\\
&\lesssim \int_0^{\delta}\int_{\mathcal{S}}\frac{(\epsilon|k|\cos\theta)r^{N+\gamma+1}}{(\nu_0 r^{1+\gamma})^2+(\epsilon r|k|\cos\theta)^2}\,\mathrm{d}r\,\mathrm{d}\mathbf{s} \\
&\lesssim \int_0^{\delta}\int_{\mathcal{S}}\frac{(\epsilon|k|\cos\theta)r^{\gamma+N+1}}{r^{\frac{2(\gamma+1)}{p}}(\epsilon r|k|\cos\theta)^{\frac{2}{q}}}\,\mathrm{d}r\,\mathrm{d}\mathbf{s}\,, \qquad (6.5)
\end{aligned}$$

where the last inequality is obtained thanks to Young's inequality with $\frac{1}{p}+\frac{1}{q}=1$. Here we have omitted all $\mathcal{O}(\epsilon^0)$ constants and we keep doing this throughout this subsection. Let us choose

$$q = 2+\eta, \quad p = \frac{2+\eta}{1+\eta}, \quad \eta>0\,, \tag{6.6}$$

then (6.5) becomes

$$\left|\frac{1}{\epsilon^{\alpha}}\left\langle\mathcal{K}(\mathcal{B}\mathcal{A}\hat{\rho})\right\rangle\right| \lesssim \int_0^{\delta}\int_{\mathcal{S}}(\epsilon|k|\cos\theta)^{1-\frac{2}{2+\eta}}r^{N-\frac{2}{2+\eta}-\frac{\eta}{\eta+2}(\gamma+1)}\,\mathrm{d}r\,, \tag{6.7}$$

where γ is defined in (2.16). Therefore, as long as we choose η small enough, we have $N-\frac{2}{2+\eta}-\frac{\eta}{\eta+2}(\gamma+1)>-1$ and

$$\lim_{\epsilon\to 0}\left|\frac{1}{\epsilon^{\alpha}}\left\langle\mathcal{K}(\mathcal{B}\mathcal{A}\hat{\rho})\right\rangle\right| = 0\,. \tag{6.8}$$

Next we look at $\mathcal{B}^3\hat{g}$:

$$\begin{aligned}\left|\frac{1}{\epsilon^\alpha}\left\langle\mathcal{K}(\mathcal{B}^3\hat{g})\right\rangle\right| &= \left|\frac{1}{\epsilon^\alpha}\left\langle\nu^{\mathbf{d}}\mathcal{B}^3\hat{g}\right\rangle\right| = \left|\frac{1}{\epsilon^\alpha}\int\nu^{\mathbf{d}}\frac{\left(\frac{\epsilon^\alpha}{\Delta t}\right)^3}{\left(\frac{\epsilon^\alpha}{\Delta t}+\nu^{\mathbf{d}}+i\epsilon v\cdot k\right)^3}\hat{g}\,\mathrm{d}v\right| \\ &\lesssim |\hat{g}|\int_{\mathrm{supp}(\hat{g})}\frac{\nu^{\mathbf{d}}\epsilon^{2\alpha}r^{N-1}}{\left[\left(\frac{\epsilon^\alpha}{\Delta t}+\nu^{\mathbf{d}}\right)^2+(\epsilon r|k|\cos\theta)^2\right]^{3/2}}\,\mathrm{d}r\,\mathrm{d}\,\mathbf{s} \\ &\lesssim \int_{\mathrm{supp}(\hat{g})}\frac{\nu^{\mathbf{d}}\epsilon^{2\alpha}r^{N-1}}{\left(\frac{\epsilon^\alpha}{\Delta t}+\nu^{\mathbf{d}}\right)^3}\,\mathrm{d}r \\ &\lesssim \int_{\mathrm{supp}(\hat{g})}\frac{\nu^{\mathbf{d}}\epsilon^{2\alpha}r^{N-1}}{\epsilon^{\frac{3\alpha}{p}}r^{\frac{3(1+\gamma)}{q}}}\,\mathrm{d}r = \int_{\mathrm{supp}(\hat{g})}\epsilon^{2\alpha-\frac{3\alpha}{p}}r^{N+\gamma-\frac{3(1+\gamma)}{q}}\,\mathrm{d}r\,, \end{aligned} \tag{6.9}$$

where the last inequality again uses Young's inequality and thus $\frac{1}{p}+\frac{1}{q}=1$. In this case we choose

$$p=\frac{3}{2}+\eta,\quad q=\frac{3+2\eta}{1+2\eta},\quad \eta>0\,,$$

and thus $N+\gamma-\frac{3(1+\gamma)}{q}>-1$ for small η. Therefore,

$$\lim_{\epsilon\to 0}\left|\frac{1}{\epsilon^\alpha}\left\langle\mathcal{K}(\mathcal{B}^3\hat{g})\right\rangle\right| = 0\,. \tag{6.10}$$

Third, we consider $\mathcal{B}^2\mathcal{C}\hat{g}$:

$$\begin{aligned}\left|\frac{1}{\epsilon^\alpha}\left\langle\mathcal{K}(\mathcal{B}^2\mathcal{C}\hat{g})\right\rangle\right| &= \left|\frac{1}{\epsilon^\alpha}\left\langle\nu^{\mathbf{d}}\mathcal{B}^2\mathcal{C}\hat{g}\right\rangle\right| = \left|\frac{1}{\epsilon^\alpha}\int\nu^{\mathbf{d}}\frac{\left(\frac{\epsilon^\alpha}{\Delta t}\right)^2}{\left(\frac{\epsilon^\alpha}{\Delta t}+\nu^{\mathbf{d}}+i\epsilon v\cdot k\right)^2}(\mathcal{C}\hat{g})dv\right| \\ &\lesssim \int_0^\delta\int_{\mathcal{S}}\frac{\nu^{\mathbf{d}}\epsilon^{\alpha}r^{N-1}}{\left(\frac{\epsilon^\alpha}{\Delta t}+\nu^{\mathbf{d}}\right)^2+(\epsilon r|k|\cos\theta)^2}\,\mathrm{d}r\|\mathcal{C}\hat{g}\|_{L^\infty_v}\,.\end{aligned}$$

Then using a similar argument to the above, we show that

$$\begin{aligned}\int_0^\delta\int_{\mathcal{S}}\frac{\nu^{\mathbf{d}}\epsilon^{\alpha}r^{N-1}}{\left(\frac{\epsilon^\alpha}{\Delta t}+\nu^{\mathbf{d}}\right)^2+(\epsilon r|k|\cos\theta)^2}\,\mathrm{d}r &\lesssim \int_0^\delta\frac{\epsilon^\alpha r^{N+\gamma}}{\left(\frac{\epsilon^\alpha}{\Delta t}+\nu_0 r^{1+\gamma}\right)^2}\,\mathrm{d}r \\ &\lesssim \int_0^\delta\frac{\epsilon^\alpha r^{N+\gamma}}{\epsilon^{\frac{2\alpha}{q}}r^{\frac{2(1+\gamma)}{p}}}\,\mathrm{d}r\,,\end{aligned}$$

where the last inequality is also from Young's inequality and we again pick p and q from (6.6). Then as long as η is small enough such that $N+\gamma-2(1+\gamma)\frac{1+\eta}{2+\eta}=N-\frac{2+2\eta}{2+\eta}-\gamma\frac{\eta}{\eta+2}>-1$, we have

$$\lim_{\epsilon\to 0}\int_0^\delta\int_{\mathcal{S}}\frac{\nu^{\mathbf{d}}\epsilon^{\alpha}r^{N-1}}{\left(\frac{\epsilon^\alpha}{\Delta t}+\nu^{\mathbf{d}}\right)^2+(\epsilon r|k|\cos\theta)^2}\,\mathrm{d}r = 0\,, \tag{6.11}$$

which along with the fact (6.3) gives rise to

$$\lim_{\epsilon\to 0}\left|\frac{1}{\epsilon^\alpha}\left\langle\mathcal{K}(\mathcal{B}^2\mathcal{C}\hat{g})\right\rangle\right| = 0\,. \tag{6.12}$$

We then take care of terms with $\mathcal{C}$. For brevity of notation, let us denote

$$\mathcal{C}f = \mathcal{G}\left\langle \nu^{\mathbf{d}} f\right\rangle, \quad \mathcal{G} = \frac{\frac{\nu^{\mathbf{d}}\mathcal{M}^{\mathbf{d}}}{\langle \nu^{\mathbf{d}}\mathcal{M}^{\mathbf{d}}\rangle} - \mathcal{M}^{\mathbf{d}}}{\frac{\epsilon^\alpha}{\Delta t} + \nu^{\mathbf{d}} + i\epsilon v\cdot k} \tag{6.13}$$

for the special choice of $\mathcal{K}$ (3.16). Now we look at $\mathcal{C}\mathcal{A}\hat{\rho}$ first.

$$\frac{1}{\epsilon^\alpha}\left\langle \mathcal{K}(\mathcal{C}\mathcal{A}\hat{\rho})\right\rangle = \frac{1}{\epsilon^\alpha}\left\langle \nu^{\mathbf{d}}\mathcal{A}\hat{\rho}\right\rangle\left\langle \nu^{\mathbf{d}}\mathcal{G}\right\rangle . \tag{6.14}$$

Noting that $\lim_{\epsilon\to 0}\frac{1}{\epsilon^\alpha}\left\langle \nu^{\mathbf{d}}\mathcal{A}\hat{\rho}\right\rangle$ is bounded from (3.24) and

$$\lim_{\epsilon\to 0}\left\langle \nu^{\mathbf{d}}\mathcal{G}\right\rangle = \lim_{\epsilon\to 0}\int \frac{\nu^{\mathbf{d}}\left(\frac{\nu^{\mathbf{d}}\mathcal{M}^{\mathbf{d}}}{\langle \nu^{\mathbf{d}}\mathcal{M}^{\mathbf{d}}\rangle} - \mathcal{M}^{\mathbf{d}}\right)}{\frac{\epsilon^\alpha}{\Delta t} + \nu^{\mathbf{d}} + i\epsilon v\cdot k}\,\mathrm{d}v = 0\,, \tag{6.15}$$

we immediately have

$$\lim_{\epsilon\to 0}\frac{1}{\epsilon^\alpha}\left\langle \mathcal{K}(\mathcal{C}\mathcal{A}\hat{\rho})\right\rangle = 0\,. \tag{6.16}$$

Likewise, we consider $\mathcal{B}\mathcal{C}^2\hat{g}$:

$$\begin{aligned}
\left|\frac{1}{\epsilon^\alpha}\left\langle \mathcal{K}(\mathcal{B}\mathcal{C}^2\hat{g})\right\rangle\right| &= \left|\frac{1}{\epsilon^\alpha}\left\langle \nu^{\mathbf{d}}\mathcal{B}\mathcal{C}^2\hat{g}\right\rangle\right| = \left|\frac{1}{\epsilon^\alpha}\int \nu^{\mathbf{d}}\frac{\frac{\epsilon^\alpha}{\Delta t}}{\frac{\epsilon^\alpha}{\Delta t} + \nu^{\mathbf{d}} + i\epsilon v\cdot k}\mathcal{G}\left\langle \nu^{\mathbf{d}}\mathcal{C}\hat{g}\right\rangle\,\mathrm{d}v\right| \\
&= \left|\int \nu^{\mathbf{d}}\frac{\frac{1}{\Delta t}}{\frac{\epsilon^\alpha}{\Delta t} + \nu^{\mathbf{d}} + i\epsilon v\cdot k}\mathcal{G}\left\langle \nu^{\mathbf{d}}\mathcal{G}\left\langle \nu^{\mathbf{d}}\hat{g}\right\rangle\right\rangle\,\mathrm{d}v\right| \\
&= \left|\left\langle \nu^{\mathbf{d}}\mathcal{G}\right\rangle\int \frac{\nu^{\mathbf{d}}/\Delta t}{\frac{\epsilon^\alpha}{\Delta t} + \nu^{\mathbf{d}} + i\epsilon v\cdot k}\mathcal{C}\hat{g}\,\mathrm{d}v\right| \\
&\lesssim \left\langle \nu^{\mathbf{d}}\mathcal{G}\right\rangle\int_{|v|\le\delta}\left|\frac{\nu^{\mathbf{d}}}{\frac{\epsilon^\alpha}{\Delta t} + \nu^{\mathbf{d}} + i\epsilon v\cdot k}\right|\,\mathrm{d}v\|\mathcal{C}\hat{g}\|_{L^\infty_v} \lesssim \left\langle \nu^{\mathbf{d}}\mathcal{G}\right\rangle .
\end{aligned} \tag{6.17}$$

Since we have (6.15), it is easy to see that

$$\lim_{\epsilon\to 0}\left|\frac{1}{\epsilon^\alpha}\left\langle \mathcal{K}(\mathcal{B}\mathcal{C}^2\hat{\rho})\right\rangle\right| = 0\,. \tag{6.18}$$

Similarly, for the term $\mathcal{B}\mathcal{C}\mathcal{A}\hat{\rho}$, we have

$$\begin{aligned}
\frac{1}{\epsilon^\alpha}\left\langle \mathcal{K}(\mathcal{B}\mathcal{C}\mathcal{A}\hat{\rho})\right\rangle &= \frac{1}{\epsilon^\alpha}\left\langle \nu^{\mathbf{d}}\mathcal{B}\mathcal{C}\mathcal{A}\hat{\rho}\right\rangle = \frac{1}{\epsilon^\alpha}\int \frac{\nu^{\mathbf{d}}\frac{\epsilon^\alpha}{\Delta t}}{\frac{\epsilon^\alpha}{\Delta t} + \nu^{\mathbf{d}} + i\epsilon v\cdot k}\mathcal{G}\left\langle \nu\mathcal{A}\hat{\rho}\right\rangle\,\mathrm{d}v \\
&= \frac{1}{\epsilon^\alpha}\left\langle \nu\mathcal{A}\hat{\rho}\right\rangle\int \frac{\nu^{\mathbf{d}}\frac{\epsilon^\alpha}{\Delta t}}{\frac{\epsilon^\alpha}{\Delta t} + \nu^{\mathbf{d}} + i\epsilon v\cdot k}\frac{\frac{\nu^{\mathbf{d}}\mathcal{M}^{\mathbf{d}}}{\langle \nu^{\mathbf{d}}\mathcal{M}^{\mathbf{d}}\rangle} - \mathcal{M}^{\mathbf{d}}}{\frac{\epsilon^\alpha}{\Delta t} + \nu^{\mathbf{d}} + i\epsilon v\cdot k}\,\mathrm{d}v\,.
\end{aligned} \tag{6.19}$$

Noting from (3.24) that $\frac{1}{\epsilon^\alpha}\left\langle \nu\mathcal{A}\hat{\rho}\right\rangle \sim \mathcal{O}(1)$ as $\epsilon\to 0$, (6.19) reduces to

$$\frac{1}{\epsilon^\alpha}\left\langle \mathcal{K}(\mathcal{B}\mathcal{C}\mathcal{A}\hat{\rho})\right\rangle \lesssim \int_{|v|\le\delta}\left|\frac{\epsilon^\alpha\nu^{\mathbf{d}}}{\left(\frac{\epsilon^\alpha}{\Delta t} + \nu^{\mathbf{d}} + i\epsilon v\cdot k\right)^2}\right|\left|\frac{\nu^{\mathbf{d}}\mathcal{M}^{\mathbf{d}}}{\langle \nu^{\mathbf{d}}\mathcal{M}^{\mathbf{d}}\rangle} - \mathcal{M}^{\mathbf{d}}\right|\,\mathrm{d}v\,. \tag{6.20}$$

Since $|\frac{\nu^{\mathbf{d}}\mathcal{M}^{\mathbf{d}}}{\langle \nu^{\mathbf{d}}\mathcal{M}^{\mathbf{d}}\rangle} - \mathcal{M}^{\mathbf{d}}|$ is an $\mathcal{O}(1)$ term, the limit of the above equation becomes zero following from (6.11).

(3) At last, we consider $\mathcal{C}^3\hat{g}$:

$$\frac{1}{\epsilon^\alpha}\left\langle \mathcal{K}(\mathcal{C}^3\hat{\rho})\right\rangle = \frac{1}{\epsilon^\alpha}\left\langle \nu^{\mathbf{d}}\mathcal{C}^3\hat{g}\right\rangle = \frac{1}{\epsilon^\alpha}\int \nu^{\mathbf{d}}\mathcal{G}\left\langle \nu^{\mathbf{d}}\mathcal{C}^2\hat{g}\right\rangle \,\mathrm{d}v$$

$$= \frac{1}{\epsilon^\alpha}\left\langle \nu^{\mathbf{d}}\mathcal{G}\right\rangle \int \nu^{\mathbf{d}}\mathcal{C}\left\langle \mathcal{C}\hat{g}\right\rangle \,\mathrm{d}v = \frac{1}{\epsilon^\alpha}\left\langle \nu^{\mathbf{d}}\mathcal{G}\right\rangle^3\left\langle \nu^{\mathbf{d}}g\right\rangle . \tag{6.21}$$

To estimate $\left\langle \nu^{\mathbf{d}}\mathcal{G}\right\rangle$ for small ϵ, recall from (6.15) that

$$\left\langle \nu^{\mathbf{d}}\mathcal{G}\right\rangle = \int_{|v|\le\delta}\frac{\nu^{\mathbf{d}}h(v)}{\frac{\epsilon^\alpha}{\Delta t}+\nu^{\mathbf{d}}+i\epsilon v\cdot k}\,\mathrm{d}v = \int_{|v|\le\delta}\frac{\nu^{\mathbf{d}}\left(\frac{\epsilon^\alpha}{\Delta t}+\nu^{\mathbf{d}}-i\epsilon v\cdot k\right)h(v)}{\left(\frac{\epsilon^\alpha}{\Delta t}+\nu^{\mathbf{d}}\right)^2+(\epsilon v\cdot k)^2}\,\mathrm{d}v$$

$$= \int_{|v|\le\delta}\frac{\nu^{\mathbf{d}}h(v)\frac{\epsilon^\alpha}{\Delta t}+(\nu^{\mathbf{d}})^2h(v)-i\epsilon v\cdot k\nu^{\mathbf{d}}h(v)}{\left(\frac{\epsilon^\alpha}{\Delta t}+\nu^{\mathbf{d}}\right)^2+(\epsilon v\cdot k)^2}\,\mathrm{d}v := I_1+I_2-iI_3\,, \tag{6.22}$$

where $h(v)=\frac{\nu^{\mathbf{d}}\mathcal{M}^{\mathbf{d}}}{\langle\nu^{\mathbf{d}}\mathcal{M}^{\mathbf{d}}\rangle}-\mathcal{M}^{\mathbf{d}}$, and we have $\|h(\cdot)\|_\infty<+\infty$ and $\int h(v)\,\mathrm{d}v=0$. Hereafter, we will assume $k\neq 0$ as the case with $k=0$ will be much easier to estimate following the same manner below. Let $\zeta=N+2+\beta$, then $\nu^{\mathbf{d}}(v)=\nu_0|v|^\zeta$, and denote $u=\frac{v}{\epsilon^{\alpha/\zeta}}$, then,

$$I_1 = \int_{|v|\le\delta}\frac{\nu^{\mathbf{d}}\frac{\epsilon^\alpha}{\Delta t}h(v)}{\left(\frac{\epsilon^\alpha}{\Delta t}+\nu^{\mathbf{d}}\right)^2+(\epsilon v\cdot k)^2}\,\mathrm{d}v$$

$$= \int_{|u|\le\frac{\delta}{\epsilon^{\alpha/\zeta}}}\frac{\nu_0|u|^\zeta h(\epsilon^{\alpha/\zeta}u)\frac{1}{\Delta t}}{\left(\frac{1}{\Delta t}+\nu_0|u|^\zeta\right)^2+\left(\epsilon^{1-\alpha+\frac{\alpha}{\zeta}}u\cdot k\right)^2}\epsilon^{\alpha N/\zeta}\,\mathrm{d}u$$

$$\lesssim \epsilon^{\alpha N/\zeta}\|h\|_\infty\int_{|u|\le\frac{\delta}{\epsilon^{\alpha/\zeta}}}\frac{|u|^\zeta}{\left(\frac{1}{\Delta t}+\nu_0|u|^\zeta\right)^2}\,\mathrm{d}u\lesssim C\epsilon^{\alpha N/\zeta}. \tag{6.23}$$

For I_2, we have

$$I_2 = \int_{|v|\le\delta}\frac{(\nu^{\mathbf{d}})^2h(v)}{\left(\frac{\epsilon^\alpha}{\Delta t}+\nu^{\mathbf{d}}\right)^2+(\epsilon v\cdot k)^2}\,\mathrm{d}v$$

$$= \int_{|v|\le\delta}\left[\frac{(\nu^{\mathbf{d}})^2h(v)}{\left(\frac{\epsilon^\alpha}{\Delta t}+\nu^{\mathbf{d}}\right)^2+(\epsilon v\cdot k)^2}-h(v)\right]\mathrm{d}v$$

$$= -\int_{|v|\le\delta}\frac{\left(\frac{\epsilon^\alpha}{\Delta t}\right)^2+2\frac{\epsilon^\alpha}{\Delta t}\nu^{\mathbf{d}}+(\epsilon v\cdot k)^2}{\left(\frac{\epsilon^\alpha}{\Delta t}+\nu^{\mathbf{d}}\right)^2+(\epsilon v\cdot k)^2}h(v)\,\mathrm{d}v\,,$$

where the first two terms can be estimated the same as for I_1 and are bounded by $C\epsilon^{\alpha N/\zeta}$. As for the third term, we have

$$\int_{|v|\le\delta}\frac{(\epsilon v\cdot k)^2h(v)}{\left(\frac{\epsilon^\alpha}{\Delta t}+\nu^{\mathbf{d}}\right)^2+(\epsilon v\cdot k)^2}\,\mathrm{d}v\le\|h(v)\|_\infty\int_{|v|\le\delta}\frac{(\epsilon v\cdot k)^2}{\left(\frac{\epsilon^\alpha}{\Delta t}+\nu^{\mathbf{d}}\right)^2+(\epsilon v\cdot k)^2}$$

$$\lesssim C\int_{|v|^\zeta\le\epsilon^\alpha}1\,\mathrm{d}v+\epsilon\int_{\epsilon^\alpha<|v|\le\delta^m}\frac{v\cdot k}{2\nu^{\mathbf{d}}}\,\mathrm{d}v$$

$$\lesssim C\epsilon^{\alpha N/\zeta}+C\epsilon\int_{\epsilon^\alpha<|v|\le\delta^m}|v|^{N-\zeta}\,\mathrm{d}|v|$$

$$\lesssim C\epsilon^{\alpha N/\zeta}+C\epsilon(1-\epsilon^{\frac{\alpha}{\zeta}(N-\zeta+1)})\le C\left(\epsilon^{\alpha N/\zeta}+\epsilon+\epsilon^{\frac{N^2+N}{\zeta}}\right).$$

Therefore,

$$I_2 \lesssim C\left(\epsilon^{\alpha N/\zeta} + \epsilon + \epsilon^{\frac{N^2+N}{\zeta}}\right). \tag{6.24}$$

For I_3, we again decompose it into two integrals,

$$\begin{aligned} I_3 &= \int_{|v|^\zeta \le \epsilon^\alpha} \frac{\epsilon v\cdot k\nu^{\mathbf{d}} h(v)}{\left(\frac{\epsilon^\alpha}{\Delta t}+\nu^{\mathbf{d}}\right)^2 + (\epsilon v\cdot k)^2}\,\mathrm{d}v \\ &\quad + \int_{\epsilon^\alpha < |v|^\zeta \le \delta^\zeta} \frac{\epsilon v\cdot k\nu^{\mathbf{d}} h(v)}{\left(\frac{\epsilon^\alpha}{\Delta t}+\nu^{\mathbf{d}}\right)^2 + (\epsilon v\cdot k)^2}\,\mathrm{d}v \\ &\le \|h(v)\|_\infty \int_{|v|^\zeta \le \epsilon^\alpha} \frac{1}{2}\,\mathrm{d}v + \|h(v)\|_\infty \int_{\epsilon^\alpha < |v|^\zeta \le \delta^\zeta} \frac{\epsilon v\cdot k}{\nu^{\mathbf{d}}}\,\mathrm{d}v \\ &\lesssim C\left(\epsilon^{\alpha N/\zeta} + \epsilon + \epsilon^{\frac{N^2+N}{\zeta}}\right). \end{aligned} \tag{6.25}$$

Combining (6.23)–(6.25), we have $\left\langle \nu^{\mathbf{d}}\mathcal{G}\right\rangle \lesssim C(\epsilon^{\alpha N/\zeta} + \epsilon + \epsilon^{\frac{N^2+N}{\zeta}})$; therefore, for big enough m, we have from (6.21) that

$$\lim_{\epsilon\to 0}\frac{1}{\epsilon^\alpha}\left\langle \mathcal{K}(\mathcal{C}^m\hat{\rho})\right\rangle = 0\,. \tag{6.26}$$

∎

To conclude, we would like to point out the following facts so that the remaining terms in (3.23) can be estimated with ease. For a general term denoted by $\mathcal{H}f$, that has been proved to admit the following limit

$$\lim_{\epsilon\to 0}\frac{1}{\epsilon^\alpha}\left\langle \mathcal{K}(\mathcal{H}f)\right\rangle = 0\,,$$

where $\mathcal{H}$ is considered as an arbitrary operator in v and x, and f can be a function of t, x, and v or just t and x, also satisfies

$$\lim_{\epsilon\to 0}\frac{1}{\epsilon^\alpha}\left\langle \mathcal{K}(\mathcal{C}^n\mathcal{H}f)\right\rangle = 0\,,\quad n\in\mathbb{Z}^+\,. \tag{6.27}$$

Indeed,

$$\frac{1}{\epsilon^\alpha}\left\langle \mathcal{K}(\mathcal{C}\mathcal{H}f)\right\rangle = \frac{1}{\epsilon^\alpha}\left\langle \nu^{\mathbf{d}}\mathcal{C}\mathcal{H}f\right\rangle = \frac{1}{\epsilon^\alpha}\left\langle \nu^{\mathbf{d}}\mathcal{G}\left\langle \nu^{\mathbf{d}}\mathcal{H}f\right\rangle\right\rangle = \frac{1}{\epsilon^\alpha}\left\langle \nu^{\mathbf{d}}\mathcal{G}\right\rangle\left\langle \nu^{\mathbf{d}}\mathcal{H}f\right\rangle$$

and, thus,

$$\lim_{\epsilon\to 0}\frac{1}{\epsilon^\alpha}\left\langle \mathcal{K}(\mathcal{C}^n\mathcal{H}f)\right\rangle = \lim_{\epsilon\to 0}\frac{1}{\epsilon^\alpha}\left\langle \nu^{\mathbf{d}}\mathcal{G}\right\rangle^n\left\langle \nu^{\mathbf{d}}\mathcal{H}f\right\rangle = 0$$

owing to (6.15). Furthermore, if f is only a function of t, x, and v and still satisfies (6.27), we also have

$$\lim_{\epsilon\to 0}\frac{1}{\epsilon^\alpha}\left\langle \mathcal{K}(\mathcal{B}^n\mathcal{H}f)\right\rangle = 0, \tag{6.28}$$

thanks to the fact (6.1).

REFERENCES

[1] N. B. Abdallah, A. Mellet, and M. Puel, *Anomalous diffusion limit for kinetic equations with degenerate collision frequency*, Math. Models Methods Appl. Sci., 21 (2011), pp. 572–601.

[2] N. B. Abdallah, A. Mellet, and M. Puel, *Fractional diffusion limit for collisional kinetic equations: A Hilbert expansion approach*, Kinet. Relat. Models, 4 (2011), pp. 873–900.

[3] C. Bardos, R. Santos, and R. Sentis, *Diffusion approximation and computation of the critical size*, Trans. Amer. Math. Soc., 284 (1984), pp. 617–649.

[4] G. Basile, S. Olla, and H. Spohn, *Energy transport in stochastically perturbed lattice dynamics*, Arch. Ration. Mech. Anal., 195 (2010), pp. 171–203.

[5] D. Benedetto, E. Caglioti, and M. Pulvirenti, *A non-Maxwellian steady distribution for one-dimensional granular media*, J. Stat. Phys., 91 (1998), pp. 979–990.

[6] A. Bensoussan, J. L. Lions, and G. Papanicolaou, *Boundary layers and homogenization of transport processes*, Publ. Res. Inst. Math. Sci., 15 (1979), pp. 53–157.

[7] A. V. Bobylev, J. A. Carrillo, and I. M. Gamba, *On some properties of kinetic and hydrodynamic equations for inelastic interactions*, J. Stat. Phys., 98 (2000), pp. 743–773.

[8] A. V. Bobylev and I. M. Gamba, *Boltzmann equations for mixtures of Maxwell gases: Exact solutions and power like tails*, J. Stat. Phys., 124 (2006), pp. 497–516.

[9] N. Crouseilles, H.Hivert, and M. Lemou, *Numerical schemes for kinetic equations in the anomalous diffusion limit. Part* II: *Degenerate collision frequency*, SIAM J. Sci. Comput., 38 (2016), pp. A2464–A2491.

[10] N. Crouseilles, H.Hivert, and M. Lemou, *Numerical schemes for kinetic equations in the anomalous diffusion limit. Part* I: *The case of heavy-tailed equilibrium*, SIAM J. Sci. Comput., 38 (2016), pp. A737–A764.

[11] P. Degond, T. Goudon, and F. Poupaud, *Diffusion limit for non homogeneous and non-micro-reversibles processes*, Indiana Univ. Math. J., 49 (2000), pp. 1175–1198.

[12] D. Duering and G. Toscani, *Anomalous diffusion limit induced on a kinetic equation*, Phys. A, 384 (2007), pp. 493–506.

[13] M. H. Ernst and R. Brito, *Scaling solutions of inelastic Boltzmann equations with over-populated high energy tails*, J. Stat. Phys., 109 (2002), pp. 407–432.

[14] M. Frank and W. Sun, *Fractional diffusion limits of non-classical transport equations*, Kinet. Relat. Models, 11 (2018), pp. 1503–1526.

[15] F. Golse, S. Jin, and C. D. Levermore, *The convergence of numerical transfer schemes in diffusive regimes* I: *Discrete-ordinate method*, SIAM J. Numer. Anal., 36 (1999), pp. 1333–1369, https://doi.org/10.1137/S0036142997315986.

[16] S. Jin, *Efficient asymptotic-preserving (AP) schemes for some multiscale kinetic equations*, SIAM J. Sci. Comput., 21 (1999), pp. 441–454.

[17] S. Jin, *Asymptotic preserving (AP) schemes for multiscale kinetic and hyperbolic equations: A review*, Riv. Math. Univ. Parma (N.S.), 3 (2012), pp. 177–216.

[18] E. W. Larsen and J. B. Keller, *Asymptotic solution of neutron transport problems for small mean free path*, J. Math. Phys., 15 (1974), pp. 75–81.

[19] A. Mellet, *Fractional diffusion limit for collisional kinetic equations: A moments method*, Indiana Univ. Math. J., 59 (2010), pp. 1333–1360.

[20] A. Mellet, S. Mischler, and C. Mouhot, *Fractional diffusion limit for collisional kinetic equations*, Arch. Ration. Mech. Anal., 199 (2011), pp. 493–525.

[21] F. Poupaud, *Diffusion approximation of the linear semiconductor Boltzmann equation: Analysis of boundary layers*, Asymptot. Anal., 4 (1991), pp. 293–317.

[22] D. Summers and R. M. Thorne, *The modified plasma dispersion function*, Phys. Fluids., 83 (1991), pp. 1835–1847.

[23] C. Villani, *Mathematics of granular materials*, J. Stat. Phys., 124 (2006), pp. 781–822.

[24] L. Wang and B. Yan, *An asymptotic preserving scheme for linear kinetic equation with fractional diffusion limit*, J. Comput. Phys., 312 (2016), pp. 157–174.

[25] B. Yan and S. Jin, *A successive penalty-based asymptotic-preserving scheme for kinetic equations*, SIAM J. Sci. Comput., 35 (2013), pp. A150–A172.